BORDERED FLOER HOMOLOGY
OF $(2, 2n)$-TORUS LINK COMPLEMENT

JAEPIL LEE

BORDERED FLOER HOMOLOGY
OF (2, 2n)-TORUS LINK COMPLEMENT

JAEPIL LEE

We compute the bordered Floer homology $\widehat{CFDD}$ of the (2, 2n)-torus link complement and discuss assorted examples and type-*DD* structure homotopy equivalence.

1. Introduction

In recent years, Heegaard Floer theory has fascinated many low-dimensional topologists. Developed by P. Ozsváth and Z. Szábo, Heegaard Floer invariants of closed three-manifolds led to a breakthrough in low dimensional topology. These invariants were recently shown to be equivalent to three-dimensional Seiberg–Witten Floer homology by Kutluhan, Lee and Taubes [Kutluhan et al. 2011]. They were also proven to be equivalent to contact homology by Colin, Ghiggini and Honda [Colin et al. 2011]; this equivalence had initially motivated Oszváth and Szabó's constructions. Moreover, Heegaard Floer theory turned out to be useful in defining knot and link invariants; see [Ozsváth and Szabó 2004a; 2008a; Rasmussen 2002]. These invariants are now known as *knot Floer homology* and *link Floer homology*. In particular, knot Floer homology and Heegaard Floer homology of a three-manifold obtained by integral surgery on knot turned out to be closely related; see [Rasmussen 2002; Ozsváth and Szabó 2008b]. For the link surgery case, the relation was discovered but appeared more complicated than the knot case; see [Manolescu and Ozsváth 2010].

More recently, Lipshitz, Ozsváth and Thurston extended the theory to three-manifolds with nonempty boundary. *Bordered Floer homology*, first introduced in [Lipshitz et al. 2008], consists of two different modules: $\widehat{CFD}$ and $\widehat{CFA}$. The homotopy type of each module is a topological invariant of a three-manifold with *connected* boundary equipped with a framing (a diffeomorphism to a model surface). The bordered theory is a powerful tool thanks to the pairing theorem: one can recover the Heegaard Floer homology of a closed 3-manifold decomposed into two pieces by taking "$\mathcal{A}_\infty$-tensor product" of $\widehat{CFA}$ of the first piece and $\widehat{CFD}$ of the second piece.

Moreover, Lipshitz, Ozsváth and Thurston [Lipshitz et al. 2015] have generalized bordered Floer homology to *doubly bordered Floer homology*. As the name suggests, this is an invariant associated to a three-manifold with two boundary components; we get three different types of bimodules, $\widehat{CFDA}$, $\widehat{CFDD}$, and $\widehat{CFAA}$. These bimodules are orginally invented to compute the bordered Floer homology of three-manifold with different framings. However, the doubly bordered Floer homology also provides an elegant algorithm to the compute Heegaard Floer homology of a closed three-manifold [Lipshitz et al. 2014], independent of the previously known combinatoric approach [Sarkar and Wang 2010].

In this paper, we give a calculation of $\widehat{CFDD}(S^3 \setminus \nu(L))$, where L is $(2, 2n)$-torus link. For a number of reasons, we mainly focus on the $\widehat{CFDD}$ module. First, it is the easiest bimodule to compute since it does not involve any $\mathcal{A}_\infty$-structure. Second, it is always possible to convert the $\widehat{CFDD}$ module to $\widehat{CFDA}$ or $\widehat{CFAA}$, by attaching the $\widehat{CFAA}(\mathbb{I})$ module to the left or right side of the $\widehat{CFDD}$ module. In Section 2, we collect the necessary background and notation. The actual calculation is in Section 3; the answer is shown in Proposition 3.9. (See also Figure 6 for a $(2, 6)$-torus link case.) The simplified version of the answer is in Figure 8. We work with a specific Heegaard diagram in order to find the generators and differentials of the module explicitly. However, only a few of the differentials can be obtained by the direct examination of their domains; for the remaining differentials, we have to exploit the A_∞-structure of $\widehat{CFAA}$. In Section 4, we give several applications of the pairing formula, recovering some known Floer homologies from our calculation, to illustrate and check the result.

Some other calculations of bordered invariants for manifolds with disconnected boundaries were recently obtained by Jonathan Hanselman [2016]. Hanselman computes the $\widehat{CFD}$-type trimodule associated to the trivial S^1-bundle over a pair of pants, and uses this, together with certain features of the bordered theory, to recover Heegaard Floer invariants of all graph manifolds. In principle, our results can also be obtained via Hanselman's approach (although he does not perform this calculation); however, our calculations are based on a more direct examination of the $(2, 2n)$ link complement, and thus it is perhaps more useful for understanding the bordered theory of more general link complements.

2. Background on doubly bordered Floer theory

We will assume that the reader is familiar with bordered Floer homology of a single boundary case. If not, we suggest the reader refer to [Lipshitz et al. 2011] for a brief introduction to the topic. In this section, we list the definitions and important results that will be used in the rest of the paper.

Algebraic preliminaries. Throughout this paper, we will use $\mathbb{F}$ to refer to $\mathbb{F}_2$.

We first begin with the algebra associated to a boundary surface of a three-manifold. In a handle decomposition of a genus g surface Σ^g, the zero-handle D of Σ^g has $2g$ marked points $\boldsymbol{a}$ on $\partial D = Z$ equipped with a two-to-one matching M between the points so that each one-handle is attached to a pair of matched points. We also fix a point z on Z away from $\boldsymbol{a}$. This set of data is called a *pointed matched circle* and denoted by

$$\mathcal{Z} = \{Z, \boldsymbol{a}, M, z\}.$$

$F(\mathcal{Z})$ denotes the surface obtained by the data and $D \subset F(\mathcal{Z})$ is called a *preferred disk*. The bordered Floer package associates a *dg* algebra to $\mathcal{Z}$, which will be a *strands algebra*, and denoted by $\mathcal{A}(\mathcal{Z})$.

Since we will be studying the torus boundary case, from now on we will assume that the genus g of the boundary surface equals one. In this case, $\mathcal{A}(\mathcal{Z})$ is $\mathbb{F}_2$-vector space generated by Reeb chords ρ_I, $I \in \{1, 2, 3, 12, 23, 123\}$ and two idempotents ι_1 and ι_2 such that $\iota_1 + \iota_2 = 1$. The multiplication rule between Reeb chords follows the concatenation rule of labels of chords; that is, $\rho_I \cdot \rho_J = \rho_{IJ}$ where $I, J \in \{1, 2, 3, 12, 23, 123\}$ and IJ is the concatenation of I and J. (If IJ is not in that set, then their product is zero.) For idempotents, $\iota_1 \rho_I = \rho_I$ if I starts with 1 or 3, $\rho_I \iota_1 = \rho_I$ if I ends with 2, $\iota_2 \rho_I = \rho_I$ if I starts with 2, and $\rho_I \iota_2 = \rho_I$ if I ends with 1 or 3. We let $\mathcal{I} \subset \mathcal{A}(\mathcal{Z})$ denote the subalgebra generated by idempotents ι_1 and ι_2. This strands algebra is called a *torus algebra*. A detailed description can be found in [Lipshitz et al. 2008, Chapter 3].

Next, we will study a (right) $\mathcal{A}_\infty$-*module* and a (left) *type-D module*. For an $\mathcal{A}_\infty$-algebra (A, μ_i), an $\mathcal{A}_\infty$-module is a $\mathbb{F}$-module M, equipped with maps

$$m_i : M \otimes A^{\otimes(i-1)} \to M$$

satisfying compatibility relations

$$0 = \sum_{i+j=n+1} m_i \big(m_j(\boldsymbol{x} \otimes a_1 \otimes \cdots \otimes a_{j-1}) \otimes \cdots \otimes a_{n-1} \big)$$

$$+ \sum_{i+j=n+1} \sum_{l=1}^{n-j} m_i \big(\boldsymbol{x} \otimes a_1 \otimes \cdots \otimes a_{l-1} \otimes \mu_j(a_l \otimes \cdots \otimes a_{l+j-1}) \otimes \cdots \otimes a_{n-1} \big),$$

for all $i \geq 1$. An $\mathcal{A}_\infty$-module is *strictly unital* if

$$m_2(\boldsymbol{x} \otimes 1) = \boldsymbol{x} \quad \text{and} \quad m_i(\boldsymbol{x} \otimes a_1 \otimes \cdots \otimes a_{i-1}) = 0 \text{ for } i > 2 \text{ and some } a_j = 1.$$

In bordered Floer theory, an $\mathcal{A}_\infty$-module is called a *type-A* module.

For a *dg*-algebra (A, μ_1, μ_2), a type-D module is a $\mathbb{F}$-module equipped with a map $\delta^1 : N \to A \otimes N$, satisfying the compatibility relation

$$0 = (\mu_2 \otimes \mathbb{I}_N) \circ (\mathbb{I}_A \otimes \delta^1) \circ \delta^1 + (\mu_1 \otimes \mathbb{I}_N) \circ \delta^1.$$

These modules are generalized to the following bimodules, namely a *type-AA bimodule* and a *type-DD bimodule*. In this paper, we will be mainly studying these bimodules.

Definition 2.1. Let A and B be $\mathcal{A}_\infty$-algebras over $\mathbb{F}$ equipped with $\mathcal{A}_\infty$-maps $\{\mu_i^A\}_{i>0}$ and $\{\mu_i^B\}_{i>0}$, respectively. A *right-right $\mathcal{A}_\infty$-bimodule* of *type-AA bimodule* $M_{\mathcal{A},\mathcal{B}}$ over A and B consists of a right-right $(\mathbb{F}, \mathbb{F})$-bimodule M and maps
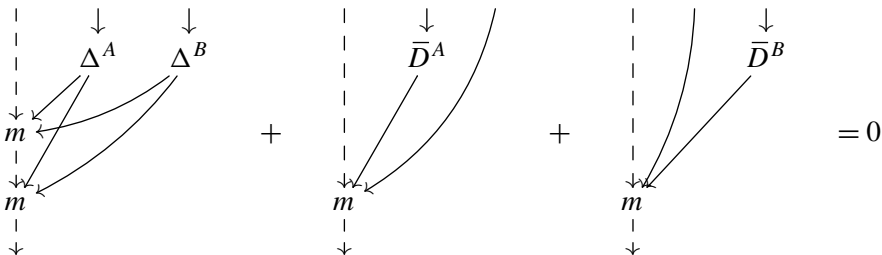
$$m_{1,i,j} : M \otimes A^{\otimes i} \otimes B^{\otimes j} \to M$$

such that the following compatibility condition holds.

$$0 = \sum_{\substack{k+l=i \\ \lambda+\eta=j}} m_{1,k,\lambda}\big(m_{1,l,\eta}(\boldsymbol{x}, a_1 \otimes \cdots \otimes a_l, b_1 \otimes \cdots \otimes b_\eta), a_{l+1} \otimes \cdots \otimes a_i, b_{\eta+1} \otimes \cdots \otimes b_j\big)$$

$$+ \sum_{k+l=i+1} \sum_{n=1}^{i-l+1} m_{1,k,j}\big(\boldsymbol{x}, a_1 \otimes \cdots \otimes a_{n-1} \otimes \mu_l^A(a_n \otimes \cdots \otimes a_{n+l-1}) \otimes \cdots \otimes a_i,$$
$$b_1 \otimes \cdots \otimes b_j\big)$$

$$+ \sum_{\lambda+\eta=j+1} \sum_{n=1}^{j-\eta+1} m_{1,i,\lambda}\big(\boldsymbol{x}, a_1 \otimes \cdots \otimes a_i,$$
$$b_1 \otimes \cdots \otimes b_{n-1} \otimes \mu_\eta^B(b_n \otimes \cdots \otimes b_{n+l-1}) \otimes \cdots \otimes b_j\big)$$

for all $i \geq 0$ and $j \geq 0$.

By writing $m = \sum_{i,j} m_{1,i,j}$, the compatibility condition can be drawn as the diagram below.

The dashed line above represents a module element, and the regular line represents an element from tensor algebra $\mathcal{T}^*A$ and $\mathcal{T}^*B$. The map $\Delta^A : \mathcal{T}^*A \to \mathcal{T}^*A \otimes \mathcal{T}^*A$ represents the canonical comultiplication

$$\Delta^A(a_1 \otimes \cdots \otimes a_n) = \sum_{m=0}^{n} (a_1 \otimes \cdots \otimes a_m) \otimes (a_{m+1} \otimes \cdots \otimes a_n),$$

and $\bar{D}^A : \mathcal{T}^*A \to \mathcal{T}^*A$ is defined as

$$\bar{D}^A(a_1 \otimes \cdots \otimes a_n) = \sum_{j=1}^{n} \sum_{l=1}^{n-j+1} a_1 \otimes \cdots \otimes \mu_j^A(a_l \otimes \cdots \otimes a_{l+j-1}) \otimes \cdots \otimes a_n.$$

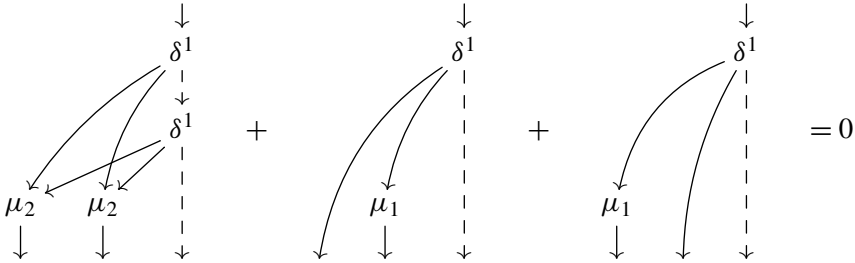Δ^B and $\bar{D}^B$ are defined similarly.

Definition 2.2. Let A and B be $\mathcal{A}_\infty$-algebras over $\mathbb{F}$. A *left-left type-DD bimodule* $^{A,B}M$ over A and B consists of left-left $(\mathbb{F}, \mathbb{F})$-bimodule M and maps

$$\delta^1 : M \to A \otimes B \otimes M$$

satisfying the following compatibility condition.

$$((\mu_2^L, \mu_2^R) \otimes \mathbb{I}_M) \circ ((\mathbb{I}_A, \mathbb{I}_B) \otimes \delta^1) \circ \delta^1 + ((\mu_1^L, \mathbb{I}_B) \otimes \mathbb{I}_M) \circ \delta^1 + ((\mathbb{I}_A, \mu_1^R) \otimes \mathbb{I}_M) \circ \delta^1 = 0.$$

Again, the compatibility condition is drawn as the diagram below.

Heegaard diagram of the bordered three-manifold. A *bordered three-manifold* is a quadruple $(Y_1, \Delta_1, z_1, \psi_1)$, where Y_1 is a three-manifold with boundary, Δ_1 is a disk in ∂Y_1, z_1 is a point in $\partial \Delta_1$, and $\psi_1 : (F(\mathcal{Z}), D, z) \to (\partial Y_1, \Delta_1, z_1)$ is a parametrization of boundary. That is, ψ is a homeomorphism from $F(\mathcal{Z})$ to ∂Y_1 sending D to Δ_1 and z to z_1.

To describe a bordered three-manifold, we use a *bordered Heegaard diagram*.

Definition 2.3. A *bordered Heegaard diagram* is a quadruple $\mathcal{H} = (\bar{\sigma}, \bar{\boldsymbol{\alpha}}, \boldsymbol{\beta}, z)$ consisting of

- a compact, oriented surface $\bar{\sigma}$ of genus g with a single boundary component;
- a g-tuple of disjoint circles $\boldsymbol{\beta} = \{\beta_1, \ldots, \beta_g\}$ in the interior of $\bar{\sigma}$;

- a $g + k$-tuple of disjoint curves $\overline{\boldsymbol{\alpha}} = \boldsymbol{\alpha}^c \cup \boldsymbol{\alpha}^a$ in $\bar{\sigma}$, where $\boldsymbol{\alpha}^c = \{\alpha_1^c, \ldots, \alpha_{g-k}^c\}$ is a set of circles in the interior of $\bar{\sigma}$, and $\boldsymbol{\alpha}^a = \{\alpha_1^a, \ldots, \alpha_{2k}^a\}$ is a set of arcs whose boundaries are in $\partial\bar{\sigma}$;

- a point z in $\partial\bar{\sigma}$, away from the boundaries of arcs in $\boldsymbol{\alpha}^a$,

such that $\bar{\sigma}\backslash\overline{\boldsymbol{\alpha}}$ and $\bar{\sigma}\backslash\boldsymbol{\beta}$ are connected, and $\overline{\boldsymbol{\alpha}}$ and $\boldsymbol{\beta}$ intersect transversally.

We construct a bordered three-manifold from a bordered Heegaard diagram $\mathcal{H}$ in the following manner. First, we obtain a three-manifold with boundary $Y(\mathcal{H})$ by thickening $\bar{\sigma} \times [0, 1]$ and attaching a three-dimensional two-handle to each $\alpha_i^c \times \{0\} \times \bar{\sigma}$ and a three-dimensional two-handle to each $\beta_i \times \{1\} \times \bar{\sigma}$. The boundary of the resulting manifold is a genus k surface, and the surface is decomposed into a disk D and a genus k surface with a single boundary by $\partial\bar{\sigma} \times \{1\}$. Then, we get a bordered three-manifold $(Y(\mathcal{H}), D, z, \psi)$, where ψ is determined by $\boldsymbol{\alpha}^a$, which is considered as parametrization data of the surface.

A bordered Floer package defines a type-D module $\widehat{CFD}(\mathcal{H})$ and a type-A module $\widehat{CFA}(\mathcal{H})$ from a bordered Heegaard diagram $\mathcal{H}$, which are well defined up to quasi-isomorphism. Each module has a generating set $\mathfrak{S}(\mathcal{H})$, whose element $\boldsymbol{x} = \{x_1, \ldots, x_g\}$ is a g-tuple of points in $\bar{\sigma}$ such that

- exactly one x_i lies on each β-circle,

- exactly one x_i lies on each α-circle and

- at most one x_i lies on each α-arc.

To compute nontrivial differentials for the Floer theory, we will need to compute holomophic curves in $\bar{\sigma} \times I_s \times \mathbb{R}_t$, where $I_s = [0, 1]$ with parameter s and $\mathbb{R}_t$ is $\mathbb{R}$ with parameter t. We will consider curves whose boundaries are on $\overline{\boldsymbol{\alpha}} \times \{1\} \times \mathbb{R}_t$ and $\boldsymbol{\beta} \times \{0\} \times \mathbb{R}_t$, asymptotic to $\boldsymbol{x} \times I_s$ and $\boldsymbol{y} \times I_s$ at $t = \pm\infty$ for $\boldsymbol{x}, \boldsymbol{y} \in \mathfrak{S}(\mathcal{H})$. Each of the curves carries a relative homology class in the relative homology group

$$H_2\big(\bar{\sigma} \times I_s \times [-\infty, +\infty], ((\overline{\boldsymbol{\alpha}} \times \{1\} \cup \boldsymbol{\beta} \times \{0\} \cup ((\partial\bar{\sigma}\backslash z) \times I_s)) \times [-\infty, +\infty])$$

$$\cup ((\boldsymbol{x} \times I_s \times \{-\infty\}) \cup (\boldsymbol{y} \times I_s \times \{+\infty\}))\big).$$

We write $\pi_2(\boldsymbol{x}, \boldsymbol{y})$ as the set of these relative homology classes.

Note that for $B \in \pi_2(\boldsymbol{x}, \boldsymbol{y})$, projecting B onto $\bar{\sigma}$ gives an element in $H_2(\bar{\sigma}, \overline{\boldsymbol{\alpha}} \cup \boldsymbol{\beta} \cup \partial\bar{\sigma})$. This is a linear combination of components of $\bar{\sigma}\backslash(\overline{\boldsymbol{\alpha}} \cup \boldsymbol{\beta})$. This linear combination will be called *domain*. Typically a domain is written as a linear combination of regions (connected subset of $\bar{\sigma}\backslash(\overline{\boldsymbol{\alpha}} \cup \boldsymbol{\beta})$). In particular, if any $B \in \pi_2(\boldsymbol{x}, \boldsymbol{y})$ is meeting $(\partial\bar{\sigma}\backslash z) \times I_s \times [-\infty, +\infty]$, then it can be interpreted as the corresponding domain being adjacent to the boundary of $\bar{\sigma}$, and that gives a sequence of Reeb chords $\boldsymbol{\rho} = (\rho_1, \ldots, \rho_n)$. We call $(B, \boldsymbol{\rho})$ a *compatible pair*.

There is an operation $* : \pi_2(\boldsymbol{x}, \boldsymbol{y}) \times \pi_2(\boldsymbol{y}, \boldsymbol{z}) \to \pi_2(\boldsymbol{x}, \boldsymbol{z})$, defined by concatenating two homology classes in the t factor. In particular, if $\pi_2(\boldsymbol{x}, \boldsymbol{y})$ is nonempty, then the

action of $\pi_2(\boldsymbol{x}, \boldsymbol{x})$ on $\pi_2(\boldsymbol{x}, \boldsymbol{y})$ is free and transitive. The domain of the element in $\pi_2(\boldsymbol{x}, \boldsymbol{x})$ is called *periodic domain*. In addition, $\pi_2^{\partial}(\boldsymbol{x}, \boldsymbol{x})$ denotes a set of periodic domains not adjacent to the boundary. An element in $\pi_2^{\partial}(\boldsymbol{x}, \boldsymbol{x})$ is a *provincial periodic domain*, and if every provincial periodic domain of a Heegaard diagram has both positive and negative coefficients, then the Heegaard diagram is called *provincially admissible*.

It is worth mentioning that

- if any $B \in \pi_2(\boldsymbol{x}, \boldsymbol{y})$ represents a holomorphic curve, then all the coefficients of the domain of B must be nonnegative, and

- the operation $*$ of two classes corresponds to the sum of the respective domains.

We sometimes blur the distinction between homology classes and their domains if it does not cause confusion.

We define $\widehat{CFD}(\mathcal{H})$ as the following. Let $X(\mathcal{H})$ be the $\mathbb{F}$-module generated by $\mathfrak{S}(\mathcal{H})$ equipped with an action of $\mathcal{I} \subset \mathcal{A} = \mathcal{A}(-\mathcal{Z})$ (the negative sign means the algebra obtained from the pointed matched circle has an orientation opposite from the induced orientation of $\mathcal{H}$) such that for any idempotent $\iota \in \mathcal{I}$,

$$\iota \otimes \boldsymbol{x} := \begin{cases} \boldsymbol{x} & \text{if the arc corresponding to } \iota \text{ is not occupied by } \boldsymbol{x}, \\ 0 & \text{otherwise.} \end{cases}$$

Then $\widehat{CFD}(\mathcal{H}) := \mathcal{A} \otimes_{\mathcal{I}} X(\mathcal{H})$. Its differential δ^1 is defined as

$$\delta^1(\boldsymbol{x}) := \sum_{\boldsymbol{y} \in \mathfrak{S}(\mathcal{H})} \sum_{B \in \pi_2(\boldsymbol{x}, \boldsymbol{y})} a^B_{\boldsymbol{x}, \boldsymbol{y}} \cdot \boldsymbol{y},$$

where

$$a^B_{\boldsymbol{x}, \boldsymbol{y}} := \sum_{\{\boldsymbol{\rho} \mid \mathrm{ind}(B, \boldsymbol{\rho}) = 1\}} \#(\mathcal{M}^B(\boldsymbol{x}, \boldsymbol{y}; \boldsymbol{\rho})) a(-\boldsymbol{\rho}).$$

Here, $\mathcal{M}^B(\boldsymbol{x}, \boldsymbol{y}; \boldsymbol{\rho})$ denotes the moduli space of holomorphic curves of B representing the compatible pair $(B, \boldsymbol{\rho})$, and $\mathrm{ind}(B, \boldsymbol{\rho})$ the expected dimension of the moduli space. In addition, for $\boldsymbol{\rho} = \{\rho_1, \ldots, \rho_n\}$ a sequence of Reeb chords, $a(-\boldsymbol{\rho})$ be the product $a(-\rho_1) \cdots a(-\rho_n) \in \mathcal{A}$. (Again, the negative sign means that the orientation of the boundary $\partial\bar{\sigma}$ is opposite from the induced orientation.)

The differential δ^1 may not be well defined. In fact, there may be infinitely many homology classes in $\pi_2(\boldsymbol{x}, \boldsymbol{y})$ if there is a periodic domain representing a holomorphic curve. To prevent this, we will work on a Heegaard diagram such that every periodic domain has both positive and negative coefficients. Such diagram is called *admissible*, and it is shown in [Lipshitz et al. 2008, Proposition 4.25] that every Heegaard diagram is isotopic to an admissible Heegaard diagram. (In fact, the provincial admissibility also ensures the sum is finite since the concatenation of

nonprovincial periodic domains of holomorphic curves produces an algebra element that equals zero.)

The definition of $\widehat{CFA}(\mathcal{H})$ is similar. $\widehat{CFA}(\mathcal{H})$ is a $\mathbb{F}$-module generated by $\mathfrak{S}(\mathcal{H})$, equipped with an action of $\mathcal{I} \subset \mathcal{A}(\mathcal{Z})$ such that

$$
\boldsymbol{x} \otimes \iota := \begin{cases} \boldsymbol{x} & \text{if the arc corresponding to } \iota \text{ is occupied by } \boldsymbol{x}, \\ 0 & \text{otherwise}. \end{cases}
$$

$\widehat{CFA}(\mathcal{H})$ is $\mathbb{F}$-module $X(\mathcal{H})$ generated by $\mathfrak{S}$, equipped with the $\mathcal{A}_\infty$-module maps

$$
m_{i+1} : X(\mathcal{H}) \otimes \underbrace{\mathcal{A}(\mathcal{Z}) \otimes \cdots \otimes \mathcal{A}(\mathcal{Z})}_{i\text{-times}} \to X(\mathcal{H})
$$

such that

$$
m_{n+1}(\boldsymbol{x}, \rho_1, \ldots, \rho_n) := \sum_{\boldsymbol{y} \in \mathfrak{S}(\mathcal{H})} \sum_{\substack{B \in \pi_2(\boldsymbol{x}, \boldsymbol{y}) \\ \mathrm{ind}(B, \boldsymbol{\rho}) = 1}} \#(\mathcal{M}^B(\boldsymbol{x}, \boldsymbol{y}; \boldsymbol{\rho})) \, \boldsymbol{y},
$$

$$
m_2(\boldsymbol{x}, 1) := \boldsymbol{x},
$$

$$
m_{n+1}(\boldsymbol{x}, \ldots, 1, \ldots) := 0, \quad n > 1.
$$

Although these modules are defined via a specific Heegaad diagram $\mathcal{H}$, it turns out the homotopy type of these modules are well defined. Thus, they are modules defined on bordered three-manifold (with single boundary).

Doubly bordered three-manifold. The bordered three-manifold is easily extended to a three-manifold with two boundary components. A *doubly bordered three-manifold* has the following data; $(Y_{12}, \Delta_1, \Delta_2, z_1, z_2, \psi_1, \psi_2, \gamma)$. Y_{12} is an oriented three-manifold with boundary $F(\mathcal{Z}_1) \sqcup F(\mathcal{Z}_2)$, Δ_i is a preferred disk of surface $F(\mathcal{Z}_i)$, z_i is a point on $\partial \Delta_i$, and ψ_i is a parametrization of $F(\mathcal{Z}_i)$, $i = 1, 2$. Moreover, γ is an arc connecting z_1 and z_2, equipped with a framing pointing into Δ_i.

A doubly bordered three-manifold can be realized by a Heegaard diagram with two boundaries, namely *arced bordered Heegaard diagram with two boundaries*.

Definition 2.4. An *arced bordered Heegaard diagram $\mathcal{H}$ with two boundaries* is a tuple $(\Sigma, \overline{\boldsymbol{\alpha}}, \boldsymbol{\beta}, z)$ satisfying:

- $\overline{\sigma}$ is a compact, genus g surface with two boundary components $\partial_L \overline{\sigma}$ and $\partial_R \overline{\sigma}$;
- $\boldsymbol{\beta}$ is g-tuple of pairwise disjoint curves in the interior of $\overline{\sigma}$;
- $\overline{\boldsymbol{\alpha}} = \{\boldsymbol{\alpha}^{a,L} = \{\alpha_1^{a,L}, \ldots, \alpha_{2l}^{a,L}\}, \boldsymbol{\alpha}^{a,R} = \{\alpha_1^{a,R}, \ldots, \alpha_{2r}^{a,R}\}, \boldsymbol{\alpha}^c = \{\alpha_1^c, \ldots, \alpha_{g-l-r}^c\}\}$, is a collection of pairwise disjoint embedded arcs with boundary on $\partial_L \overline{\sigma}$ (the $\alpha_i^{a,L}$), arcs with boundary on $\partial_R \overline{\sigma}$ (the $\alpha_i^{a,R}$), and circles (the α_i^c) in the interior of $\overline{\sigma}$;
- z is a path in $\overline{\sigma} \backslash (\overline{\boldsymbol{\alpha}} \cup \boldsymbol{\beta})$ between $\partial_L \overline{\sigma}$ and $\partial_R \overline{\sigma}$,

such that $\overline{\boldsymbol{\alpha}}$ intersects $\boldsymbol{\beta}$ transversely, and $\overline{\sigma} \backslash \overline{\boldsymbol{\alpha}}$ and $\overline{\sigma} \backslash \boldsymbol{\beta}$ are connected.

Since there are two boundaries, we have two pointed matched circles. These are

$$\mathcal{Z}_L(\mathcal{H}) = (\partial_L \bar{\sigma}, \boldsymbol{\alpha}^{a,L} \cap \partial_L \bar{\sigma}, M_L, z \cap \partial_L \bar{\sigma}),$$
$$\mathcal{Z}_R(\mathcal{H}) = (\partial_R \bar{\sigma}, \boldsymbol{\alpha}^{a,R} \cap \partial_R \bar{\sigma}, M_R, z \cap \partial_R \bar{\sigma}).$$

The construction of a doubly bordered three-manifold is similar to the construction of a single boundary case. For an arced bordered Heegaard diagram $\mathcal{H}$, cut open the diagram along the arc z. The resulting diagram is a bordered Heegaard diagram with a single boundary, which will be written as $\mathcal{H}_{dr}$. Then, construct a bordered three-manifold $Y(\mathcal{H}_{dr})$. The boundary of $Y(\mathcal{H}_{dr})$ is a surface that can be decomposed as a connected sum $F(\mathcal{Z}_L) \# F(\mathcal{Z}_R)$. Finally, attach a three-dimensional two-handle along the connect sum annulus.

The three-manifold $Y(\mathcal{H}) := Y(\mathcal{H}_{dr}) \cup \{\text{two-handle}\}$ has the following properties.

- It has two boundary surfaces $F(\mathcal{Z}_L)$ and $F(\mathcal{Z}_R)$ with parametrization given by $\boldsymbol{\alpha}^{a,L}$ and $\boldsymbol{\alpha}^{a,R}$, respectively.

- Each boundary surface has a preferred disk bounded by $\partial_L \bar{\sigma}$ or $\partial_R \bar{\sigma}$.

- Cutting open the Heegaard diagram $\mathcal{H}$ would result in two arcs z^+ and z^- on the deleted neighborhood of z. Then, the arc z^+, thought as a subset of the boundary of $Y(\mathcal{H}_{dr})$, is the framed arc in $Y(\mathcal{H})$ connecting z_1 and z_2.

For an arced Heegaard diagram $\mathcal{H}$, the type-DD bimodule $\widehat{CFDD}(\mathcal{H})$ is defined almost the same as in $\widehat{CFD}$. $\widehat{CFDD}(\mathcal{H})$ is a left-left $\mathbb{F}$-$\mathbb{F}$-module generated by $\mathfrak{S}(\mathcal{H}_{dr})$, equipped with two left actions of $\mathcal{I}_L \subset \mathcal{A}_L := \mathcal{A}(-\mathcal{Z}_L)$ and $\mathcal{I}_R \subset \mathcal{A}_R := \mathcal{A}(-\mathcal{Z}_R)$ such that for $\iota_L \in \mathcal{I}_L$ and $\iota_R \in \mathcal{I}_R$,

$$\iota_L \otimes \iota_R \otimes \boldsymbol{x} := \begin{cases} \boldsymbol{x} & \text{if the arc corresponding to } \iota_L \text{ and } \iota_R \text{ are not occupied by } \boldsymbol{x}, \\ 0 & \text{otherwise.} \end{cases}$$

Then $\widehat{CFDD}(\mathcal{H}) = \mathcal{A}_L \otimes \mathcal{A}_R \otimes \mathfrak{S}(\mathcal{H}_{dr})$ with the differential

$$\delta^1(\boldsymbol{x}) := \sum_{\boldsymbol{y} \in \mathfrak{S}(\mathcal{H}_{dr})} \sum_{B \in \pi_2(\boldsymbol{x}, \boldsymbol{y})} a^B_{\boldsymbol{x}, \boldsymbol{y}} \cdot \boldsymbol{y},$$

where

$$a^B_{\boldsymbol{x}, \boldsymbol{y}} := \sum_{\substack{\boldsymbol{\rho}^L, \boldsymbol{\rho}^R \\ \text{ind}(B, \boldsymbol{\rho}^L, \boldsymbol{\rho}^R) = 1}} \#(\mathcal{M}^B(\boldsymbol{x}, \boldsymbol{y}; \boldsymbol{\rho}^L, \boldsymbol{\rho}^R)) a(-\boldsymbol{\rho}^L) \otimes a(-\boldsymbol{\rho}^R).$$

Similarly, a type-AA bimodule $\widehat{CFAA}(\mathcal{H})$ is defined by a right-right $\mathbb{F}$-$\mathbb{F}$ bimodule generated by $\mathfrak{S}(\mathcal{H}_{dr})$ with right-right actions of idempotents.

$$\boldsymbol{x} \otimes \iota_L \otimes \iota_R := \begin{cases} \boldsymbol{x} & \text{if the arc corresponding to } \iota_L \text{ and } \iota_R \text{ are occupied by } \boldsymbol{x}, \\ 0 & \text{otherwise.} \end{cases}$$

The type-AA module maps are

$$m_{n+m+1}(\boldsymbol{x}, \rho_1^L, \ldots, \rho_n^L, \rho_1^R, \ldots, \rho_m^R) := \sum_{\boldsymbol{y} \in \mathfrak{S}(\mathcal{H})} \sum_{\substack{B \in \pi_2(\boldsymbol{x}, \boldsymbol{y}) \\ \mathrm{ind}(B, \rho^L, \rho^R)=1}} \#(\mathcal{M}^B(\boldsymbol{x}, \boldsymbol{y}; \rho^L, \rho^R))\,\boldsymbol{y}.$$

Lastly, the expected dimension of the moduli space of $\mathcal{M}^B(\boldsymbol{x}, \boldsymbol{y}; \rho^L, \rho^R)$, or $\mathrm{ind}(B, \rho^L, \rho^R)$ is computed by the formula below.

$$\mathrm{ind}(B, \rho^L, \rho^R) = e(B) + n_{\boldsymbol{x}}(B) + n_{\boldsymbol{y}}(B) + |\rho^L| + |\rho^R| + \iota(\rho^L) + \iota(\rho^R),$$

where $e(B)$ is *Euler measure*, $n_{\boldsymbol{x}}(B)$ sum of average of local multiplicities surrounding generator $\boldsymbol{x}$, $|\rho^L|$ number of Reeb chords in the sequence ρ^L, and $\iota(\rho^L)$ *linking number* of sequence ρ^L. In particular, if (B, ρ^L, ρ^R) is a provincial domain, then the above formula reduces to

(1) $$\mathrm{ind}(B, \rho^L, \rho^R) = e(B) + n_{\boldsymbol{x}}(B) + n_{\boldsymbol{y}}(B).$$

See [Lipshitz et al. 2008, Definition 5.11] for a detailed explanation.

Pairing theorem. The type-A module and type-D modules can be paired, which results in the classical Heegaard Floer homology of a closed three-manifold. The original pairing theorem is given in [Lipshitz et al. 2008, Theorem 1.3]. For any two three-manifolds Y_1 and Y_2 with $\partial Y_1 = F(\mathcal{Z}) = -\partial Y_2$,

$$\widehat{CFA}(Y_1) \widetilde{\otimes}_{\mathcal{A}(\mathcal{Z})} \widehat{CFD}(Y_2) \cong \widehat{CF}(Y_1 \cup_{F(\mathcal{Z})} Y_2)$$

where $\widetilde{\otimes}$ denotes the derived tensor product. The bimodule version of the pairing theorem is also given in [Lipshitz et al. 2015]. If Y_{12} is a doubly bordered three-manifold with boundary $F(\mathcal{Z}_1) \amalg F(\mathcal{Z}_2)$ and Y_1 is a bordered three-manifold with boundary $F(\mathcal{Z}_1)$, then

$$\widehat{CFD}(Y_1 \cup_{F(\mathcal{Z}_1)} Y_{12}) \cong \widehat{CFA}(Y_1) \widetilde{\otimes}_{\mathcal{A}(\mathcal{Z}_1)} \widehat{CFDD}(Y_{12}).$$

There exists many other variations of the pairing theorem. Interested readers should refer to [Lipshitz et al. 2015].

3. Computation of the bordered Floer bimodule of the $(2, 2n)$-torus link

Schubert normal form and diagram of 2-bridge link complements. As we will mainly focus on 2-bridge links, it is useful to mention *Schubert normal form* of a 2-bridge links (or knots). Let p be an even positive integer and q be an integer such that $0 < q < p$ and $\gcd(p, q) = 1$. Let us consider a circle with $2p$ marked point on its boundary. Choose a point and label it a_0. Label the other points $a_1, \ldots, a_{2p-1}$ in a clockwise direction. Then, connect a_i and a_{2p-i} with a straight
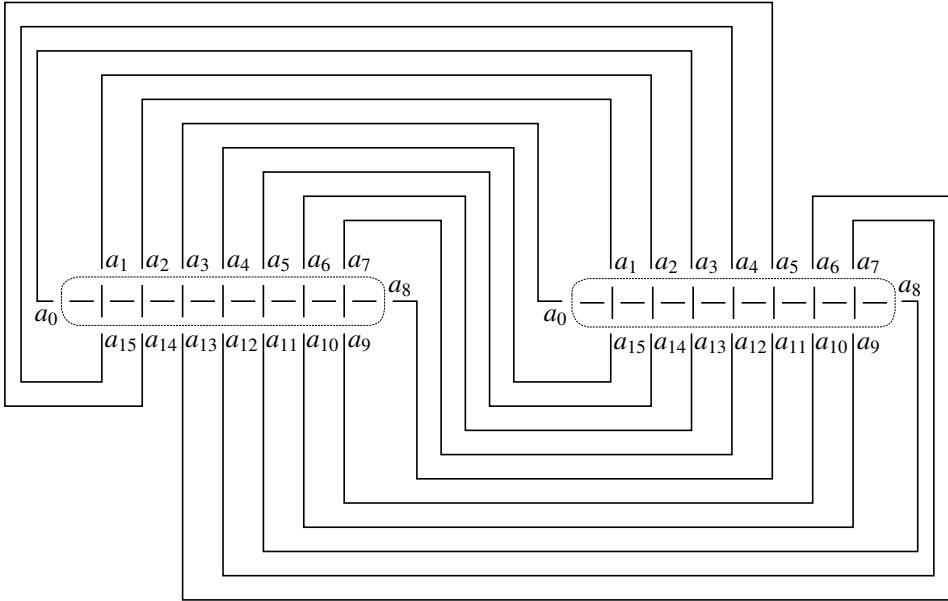
Figure 1. Schubert normal form of the $S(8, 3)$-link, or $L5a1$ in Thistlethwaite's notation.

line, $i = 1, \ldots, p - 1$. Finally, connect a_0 and a_p with an underbridge, a straight line that crosses below all of the other straight lines.

Now consider two copies of such circle. Draw arcs between these two circles so that each arc is connecting a_i on the left circle to a_{q-i} on the right circle (the labeling is modulo $2p$). These arcs should not intersect any of the straight lines and arcs. The resulting diagram gives a link that we denote $S(p, q)$. The diagram is called *Schubert normal form* of the link. See Figure 1. By construction, the diagram $S(p, q)$ has exactly two component since every even-labelled point on the right is connected to the odd-labelled point on the left (and the odd-labelled point on the right to the even-labelled point on the left). In particular, $S(2n, 1)$ is the $(2, 2n)$-torus link. More detailed description, especially about the Schubert normal form of 2-bridge knot can be found in [Rasmussen 2002, Chapter 2].

Heegaard diagram of 2-bridge link complement. Recall that a 2-bridge link L is a link in S^3 that admits a link diagram with two maxima and two minima. Let B_1 and B_2 be small neighborhoods of those two maxima. Consider

$$(S^3 \setminus \nu L) \setminus (B_1 \cup B_2).$$

Drilling a tunnel connecting B_1 and B_2 gives a three-manifold Y with single boundary, and the boundary is a genus 2 surface. Also, the longitudes λ_L and λ_R of the
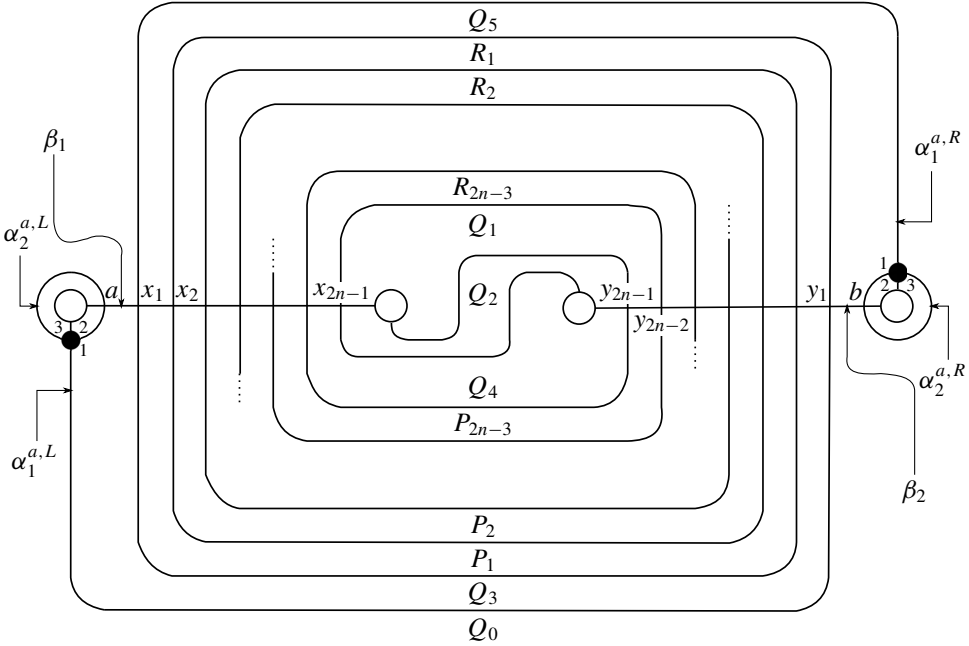
Figure 2. A general diagram of the $(2, 2n)$-torus link. The domain
Q_0 has a framed arc. The orientation on the boundaries is opposite
from the usual "right-hand" orientation.

left and right components of L are considered as curves on $\partial(\nu L)$; therefore the
longitudes are also curves on the boundary of the drilled three-manifold.

  The resulting manifold can be viewed as a handlebody with one zero-handle and
two one-handles attached to it. To get a bordered Heegaard diagram, we will apply
the following procedures on the boundary of the three-manifold. First, apply an
isotopy of the boundary surface so that the longitudes have the Schubert normal
form. Then, draw two circles β_1 and β_2 on the boundary surface so that they are
parallel to the core of the one-handles on the boundary of the one-handles. Next,
draw the meridians μ_L and μ_R on the belt sphere of each one-handle. Finally, make
two punctures at the two intersections of meridians and longitudes and relabel λ_L
to $\alpha_1^{a,L}$ and μ_L to $\alpha_2^{a,L}$ (respectively, λ_R to $\alpha_1^{a,R}$ and μ_R to $\alpha_2^{a,R}$).

  In particular, if L equals the $(2, 2n)$-torus link, then we can draw an arc z on the
surface connecting two punctures so that the arc is not intersecting $\overline{\alpha}$ or β curves.
The resulting diagram of the $(2, 2n)$-torus link complement is given in Figure 2.

Remark 3.1. Readers should be aware that connecting the left and right punctures
with an (framed) arc is not always possible. In fact, a domain that is adjacent to both
punctures does not exist except for the $(2, 2n)$-torus link case. To fix this, choose

μ_L or μ_R and apply a finger move on the chosen meridian along the longitude so that the resulting puncture is on the domain that is adjacent to the other puncture.

Computation of the type-DD module differential. Now, we compute $\widehat{CFDD}(\mathcal{H})$, where $\mathcal{H}$ is the Heegaard diagram of the $(2, 2n)$-torus link complement constructed in the previous section.

First, we will see whether the diagram $\mathcal{H}$ is provincially admissible. Second, we will investigate the genus-zero rectangular domains that cause a nontrivial differential. Then, using the result as a building block, we will consider domains of higher genus and the moduli space of homolorphic curves of the domains. The differentials associated to the higher genus domains are computed by $\mathcal{A}_\infty$-relations, dualizing $\widehat{CFDD}$-bimodule to $\widehat{CFAA}$-bimodule.

Periodic domain. First, we investigate periodic domains $\pi_2(\boldsymbol{x}, \boldsymbol{x})$. It is well known that $\pi_2(\boldsymbol{x}, \boldsymbol{x}) \cong H_2(Y(\mathcal{H}), \partial Y(\mathcal{H})) \cong \mathbb{Z} \oplus \mathbb{Z}$ by the Mayer–Vietoris sequence. Thus, there are two linearly independent periodic domains in the diagram. The proof can be found in [Lipshitz 2006, Lemma 2.6.1] or [Lipshitz et al. 2008, Lemma 4.18]. In their proof, they use the isomorphism

$$\pi_2(\boldsymbol{x}, \boldsymbol{x}) \cong H_2\big(\Sigma' \times [0, 1], (\overline{\boldsymbol{\alpha}} \times \{1\}) \cup (\boldsymbol{\beta} \times \{0\})\big),$$

where $\Sigma' = (\bar{\sigma}/\partial\bar{\sigma}) \backslash \{z\}$. The isomorphism given above is proved by investigating the long exact sequence of pair $\big(\Sigma' \times [0, 1], (\overline{\boldsymbol{\alpha}} \times \{1\}) \cup (\boldsymbol{\beta} \times \{0\})\big)$. That is,

$$\cdots \to \underbrace{H_2(\Sigma' \times [0, 1])}_{\cong 0} \to H_2\big(\Sigma' \times [0, 1], (\overline{\boldsymbol{\alpha}} \times \{1\}) \cup (\boldsymbol{\beta} \times \{0\})\big)$$
$$\to H_1\big((\overline{\boldsymbol{\alpha}} \times \{1\}) \cup (\boldsymbol{\beta} \times \{0\})\big) \to H_1(\Sigma').$$

Thus, the periodic domain $\pi_2(\boldsymbol{x}, \boldsymbol{x}) \cong \ker\big(H_1(\overline{\boldsymbol{\alpha}}/\partial\overline{\boldsymbol{\alpha}}) \oplus H_1(\boldsymbol{\beta}) \to H_1(\bar{\sigma}/\partial\overline{\Sigma})\big)$. This isomorphism enables us to find periodic domains from a bordered Heegaard diagram by choosing combinations of $\overline{\boldsymbol{\alpha}}$ and $\boldsymbol{\beta}$ curves such that the sum of their image in $H_1(\bar{\sigma}/\partial\bar{\sigma})$ equals zero. We briefly describe how to find the periodic domain from such combinations. Explicitly, first choose any orientation on the longitude $\alpha_1^{a,L}$ ($\alpha_1^{a,R}$, respectively). This induces the orientation of β_1 (β_2, respectively) as follows. For example, if the orientation of $\alpha_1^{a,L}$ is in a counterclockwise direction, then the orientation of β_1 is from right to left in the diagram. Then, we impose the coefficient zero to the outermost region that contains the framed arc. Starting from the outermost region, we give coefficients to regions adjacent to it according to the following rule. Suppose we have two adjacent regions A and B such that the coefficient of A equals l and the coefficient of B is not determined. If we can reach region B from region A by crossing a curve of multiplicity k from right to left (notion of "left" and "right" is justified since we have orientation of curves), we give the region B coefficient $k + l$; otherwise we give coefficient $-k + l$. If we can

give coefficients to all regions consistently in this way, then the orientations given
to curves $\bar{\alpha}$ and β is boundary in $H_1(\bar{\sigma}/\partial\bar{\sigma})$.

Since there are two possible choices of orientations of longitudes up to sign, we
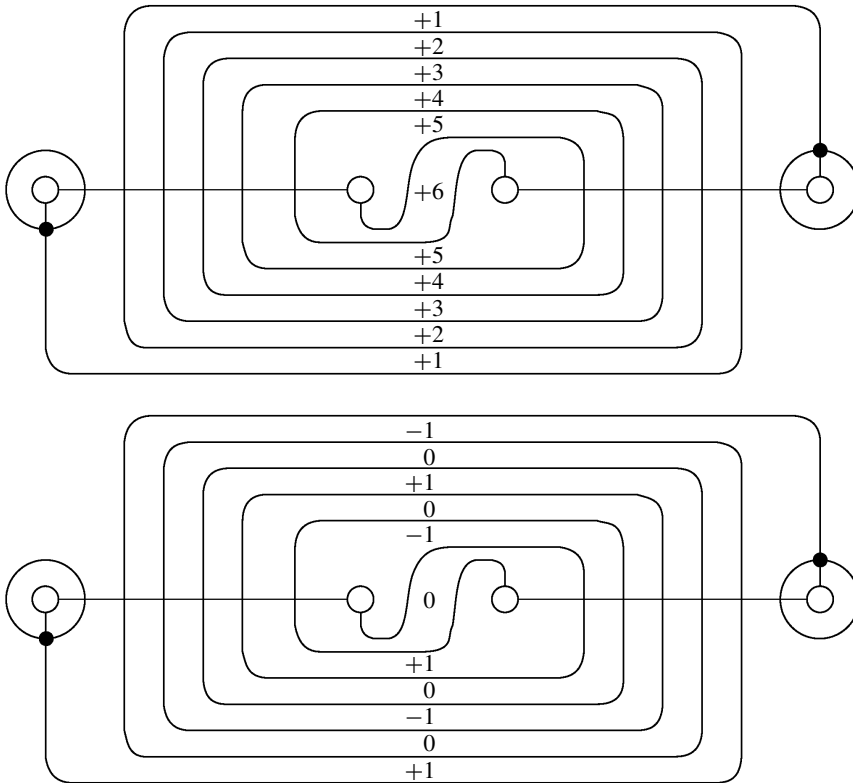find two generators of $\pi_2(x, x)$. Then the periodic domains are

$$Q_3 + Q_5 + \sum_{i=1}^{2n-3} (i+1)(P_i + R_i) + (n+2)(Q_1 + Q_4) + (n+3)Q_2$$

and

$$Q_3 - Q_5 + \sum_{i=1}^{2n-3} \frac{1+(-1)^i}{2}(P_i - R_i) + Q_4 - Q_1.$$

The two generators are shown in Figure 3.

Thus, this diagram is provincially admissible; in fact, there is no provincial
periodic domain here.

Figure 3. These two diagrams represents the two generators of
the periodic domain $\pi_2(x, x)$, where the black dots represent left
and right punctures.

Generators. According to the labeling given in the diagram, there are $2n^2 + 2n$ generators which are classified into four groups.

$$\begin{cases} x_i y_j & \text{where } i \text{ and } j \text{ have the same parity,} \\ a y_i & \text{where } i \text{ is even,} \\ x_i b & \text{where } i \text{ is even,} \\ a y_i, x_j b & \text{where } i \text{ and } j \text{ are odd.} \end{cases}$$

From now on, we will disregard generators of the last group for the following reason. The main purpose of the bordered Floer homology is to compute the Heegaard Floer homology of a three-manifold obtained by gluing along the boundaries of two three-manifolds with homeomorphic boundaries. In the link complement case, we glue the link complement and solid tori. Typically, a bordered Heegaard diagram of a solid torus is a genus one surface with a puncture, equipped with $\beta = \{\beta_1\}$ and $\overline{\alpha} = \{\alpha_1^a, \alpha_2^a\}$. In particular, these α_i^a arcs are glued to $\alpha_j^{a,L}$ or $\alpha_i^{a,R}$ of the doubly bordered diagram of the link complement, and every generator of the diagram of the solid torus is occupying exactly one α arc. Therefore, after pairing two diagrams of the solid tori to both sides of the diagram of the link complement, the generators of the last kind cannot appear in the generator set of the resulting diagram.

The differential $\delta^1 : \mathfrak{S}(\mathcal{H}) \to \mathcal{A}(-\partial_L \overline{\sigma}) \otimes \mathcal{A}(-\partial_R \overline{\sigma}) \otimes \mathfrak{S}(\mathcal{H})$ maps a generator $x \in \mathfrak{S}(\mathcal{H})$ to $\sum \rho_I \otimes \sigma_J \otimes y$, where $I, J \in \{\phi, 1, 2, 3, 12, 23, 123\}$. Here, ρ_I means an algebra element that comes from the left boundary strands algebra and σ_J, the right strands algebra. To investigate δ^1 actions on generators, it is convenient to classify the resulting terms by their strands algebra elements.

Algebra element 1. We begin by finding all provincial domains and show that only rectangular domains contribute to the differential δ^1.

Lemma 3.2. *Let (B, ρ) be a compatible pair with $\mathrm{ind}(B, \rho) = 1$. If B is a nonrectangular domain, then ρ is nonempty.*

Proof. Suppose there is a nonrectangular provincial domain B that has a nontrivial contribution to differential δ^1. Then B must be a linear combination of R_i and P_j. See Figure 2. The region covered by B must be connected, otherwise the number of corners of B will be more than four. If a domain has more than four corners then it cannot represent proper differential because the each of two generators of the differential consists of two points. Therefore, B must be an annulus. Next, we claim that the number of the corners of B must be two. This claim is justified by considering the number of corners of different types. Since the number of corners of any domain should not exceed four, there are only five possibilities, each having i 90° corners and $4 - i$ 270° corners ($i = 0, 1, 2, 3, 4$). Since the domain was assumed to be provincial, it must be a combination of the regions $P_1, \ldots, P_{2n-3}$ and $R_1, \ldots, R_{2n-3}$. Considering the index formula $e(B) + n_x(B) + n_y(B)$ of (1),

the indices of the first three cases cannot be one. Likewise, we can easily rule out the last case. The fourth case does not exist due to the following reason; because the shape of the domain is an annulus, the 270° corner must be on the boundary of the domain. Then, the other boundary must have two 90° corners. If not, i.e., if one boundary component has all three 90° corners, then there cannot be a holomorphic involution interchanging inner and outer boundaries. See [Ozsváth and Szabó 2004b, Lemma 9.4]. Thus, one boundary has two 90° corners and the other boundary has one 90° corner and one 270° corner. In particular, the boundary that has two 90° corners should consist of one $\overline{\alpha}$ curve and one β curve, and the intersections have to be 90°. However, such a boundary cannot be obtained by any combination of the domains in Figure 2. $\square$

In Figure 2, regions $P_1, \ldots, P_{2n-3}$ and $R_1, \ldots, R_{2n-3}$ are the only ones not adjacent to the boundaries. Thus, rectangular domains obtained by combining these regions are the only provincial domains. For $i = 1, \ldots, 2n-3$ and $l \leq (2n-5-i)/2$, the combinations have the form

$$P_i + \sum_{k=0}^{l} R_{i+1+2k} + P_{i+2+2k}, \quad R_i + \sum_{k=0}^{l} P_{i+1+2k} + R_{i+2+2k},$$

$$P_i + \sum_{k=0}^{l} P_{i+1+2k} + P_{i+2+2k}, \quad R_i + \sum_{k=0}^{l} R_{i+1+2k} + R_{i+2+2k}.$$

All of these domains are rectangular with four corners and each of these domains admits a unique holomorphic representative (up to translation) by the Riemann mapping theorem. The labellings of the corners tell which generators are involved. For example, the domain P_i has four corners x_i, x_{i+1}, y_{i+1} and y_{i+2}; due to the orientation convention, this domain contributes to a differential from $x_i y_{i+2}$ to $x_{i+1} y_{i+1}$. We can write the terms with algebra element 1 obtained by taking differential of $x_i y_j$:

$$(2) \qquad x_i y_j \mapsto \begin{cases} x_{j-1} y_{i+1} + x_{i+1} y_{j-1} & \text{if } j-i > 2, \\ x_{j+1} y_{i-1} + x_{i-1} y_{j+1} & \text{if } i-j > 2, \\ x_{i+1} y_{j-1} & \text{if } j-i = 2, \\ x_{i-1} y_{j+1} & \text{if } i-j = 2, \\ 0 & \text{if } i = j. \end{cases}$$

Algebra elements ρ_1 and σ_1. First, consider the algebra element ρ_1. Domain Q_3 is adjacent to the Reeb chords of algebra element ρ_1. Note that if the multiplicity of the domain Q_3 is greater than 1, then it cannot contribute to the nontrivial differential. (If so, then it will produce the algebra element $\rho_1 \cdot \rho_1$, which equals zero.) We list

the possible domains that result in nontrivial differentials:

$$Q_3 + \sum_{k=0}^{l} P_{1+2k} + P_{2+2k} \quad \text{and} \quad Q_3 + \sum_{k=0}^{l} R_{1+2k} + P_{2+2k},$$

where $l \leq n - 2$.

All such domains are rectangular domains containing Q_3. These domains are all quadrilateral, and the dimension and the modulo two count of the moduli spaces are obvious. The differentials obtained from these domains are listed below.

$$\boldsymbol{a}\boldsymbol{y}_{2k} \mapsto \begin{cases} \rho_1 \otimes (\boldsymbol{x}_1 \boldsymbol{y}_{2k-1} + \boldsymbol{x}_{2k-1} \boldsymbol{y}_1) & \text{if } k \neq 1, \\ \rho_1 \otimes \boldsymbol{x}_1 \boldsymbol{y}_1 & \text{otherwise.} \end{cases}$$

Differentials involving σ_1 can be found in a parallel manner, by using the symmetry of the diagram.

$$\boldsymbol{x}_{2k}\boldsymbol{b} \mapsto \begin{cases} \sigma_1 \otimes (\boldsymbol{x}_{2k-1} \boldsymbol{y}_1 + \boldsymbol{x}_1 \boldsymbol{y}_{2k-1}) & \text{if } k \neq 1, \\ \sigma_1 \otimes \boldsymbol{x}_1 \boldsymbol{y}_1 & \text{otherwise.} \end{cases}$$

Algebra elements ρ_3 and σ_3. Similarly, domains adjacent to ρ_3 are all listed

$$Q_1 + \sum_{k=0}^{l} R_{2n-2k-3} + R_{2n-2k-4} \quad \text{and} \quad Q_1 + \sum_{k=0}^{l} P_{2n-2k-3} + R_{2n-2k-4},$$

where $l \leq n - 2$.

Domains adjacent to σ_3 are similar. We get the differentials below:

$$\boldsymbol{a}\boldsymbol{y}_{2k} \mapsto \begin{cases} \rho_3 \otimes (\boldsymbol{x}_{2k+1} \boldsymbol{y}_{2n-1} + \boldsymbol{x}_{2n-1} \boldsymbol{y}_{2k+1}) & \text{if } k \neq n - 1, \\ \rho_3 \otimes \boldsymbol{x}_{2n-1} \boldsymbol{y}_{2n-1} & \text{otherwise;} \end{cases}$$

$$\boldsymbol{x}_{2k}\boldsymbol{b} \mapsto \begin{cases} \sigma_3 \otimes (\boldsymbol{x}_{2n-1} \boldsymbol{y}_{2k+1} + \boldsymbol{x}_{2k+1} \boldsymbol{y}_{2n-1}) & \text{if } k \neq n - 1, \\ \sigma_3 \otimes \boldsymbol{x}_{2n-1} \boldsymbol{y}_{2n-1} & \text{otherwise.} \end{cases}$$

Algebra element $\rho_2 \otimes \sigma_2$. The domain Q_2 adjacent to ρ_2 is adjacent to σ_2 as well. So, this is the one and only domain where the algebra element $\rho_2 \otimes \sigma_2$ occurs. Thus, we have $\boldsymbol{x}_{2n-1} \boldsymbol{y}_{2n-1} \mapsto \rho_2 \otimes \sigma_2 \otimes \boldsymbol{a}\boldsymbol{b}$.

Algebra elements $\rho_3 \otimes \sigma_1$ and $\rho_1 \otimes \sigma_3$. There are two domains which contribute to $\rho_3 \otimes \sigma_1$; those are $Q_1 + R_1 + R_2 + \cdots + R_{2n-3} + Q_5$ and $Q_1 + P_1 + R_2 + P_3 + R_4 + \cdots + R_{2n-4} + P_{2n-3} + Q_5$. This gives $\boldsymbol{a}\boldsymbol{b} \mapsto \rho_3 \otimes \sigma_1 \otimes (\boldsymbol{x}_1 \boldsymbol{y}_{2n-1} + \boldsymbol{x}_{2n-1} \boldsymbol{y}_1)$. Again, using the symmetry of the diagram, $\boldsymbol{a}\boldsymbol{b} \mapsto \rho_1 \otimes \sigma_3 \otimes (\boldsymbol{x}_1 \boldsymbol{y}_{2n-1} + \boldsymbol{x}_{2n-1} \boldsymbol{y}_1)$.

Now, we will work on differentials whose domains are nonrectangular. To find holomorphic curves of such domains, we will consider $\widehat{CFAA}(\mathcal{H}, 0)$ so that we can use the $\mathcal{A}_\infty$-structure of it and ensure the existence of holomorphic curves and their count (modulo two).

Algebra element containing ρ_{12}. To take advantage of the $\mathcal{A}_\infty$-structure of $\widehat{CFAA}$, the orientation of two boundaries of the Heegaard diagram has to be reversed. We let $\bar{\rho}_I$ denote (respectively, $\bar{\sigma}_I$) the algebra element of the left strands algebra $\mathcal{A}(\mathcal{Z})$ (respectively, the right strands algebra); that is, an orientation reversing diffeomorphism $R: -S^1 \backslash \{z\} \to S^1 \backslash \{z\}$ induces a map $R_*: \mathcal{A}(-\mathcal{Z}) \to \mathcal{A}(\mathcal{Z})$ that maps $R_*(\rho_1) = \bar{\rho}_3$, $R_*(\rho_2) = \bar{\rho}_2$, $R_*(\rho_3) = \bar{\rho}_1$, and so on. The right boundary is similar.

Returning to $\widehat{CFDD}$, the domains contributing to ρ_{12} must contain Q_2 and Q_3. Clearly $Q_2 + Q_3$ has more than four corners, so we will consider $Q_2 + Q_3 + Q_4$ instead to get the domain of four corners. This domain possibly contributes to the differential from $x_{2n-2}y_2$ to x_1y_1. The only possible Maslov index one interpretation is $\mathcal{M}(x_{2n-2}y_2, x_1y_1; \bar{\rho}_{23}, \bar{\sigma}_{12})$ (there can be cuts between $\bar{\rho}_2$ and $\bar{\rho}_3$, and $\bar{\sigma}_1$ and $\bar{\sigma}_2$, but these cuts will increase the Maslov index by one). Under the interpretation, the domain is an annulus with one boundary consisting of two segments of $\boldsymbol{\alpha}$ curves and two segments of $\boldsymbol{\beta}$ curves, and another boundary consisting of $\boldsymbol{\alpha}$ curve only. In the sense of [Ozsváth and Szabó 2004b, Lemma 9.4], such an annulus cannot allow a holomorphic involution that interchanges one boundary with another, carrying $\boldsymbol{\alpha}$ curves to $\boldsymbol{\alpha}$ curves and $\boldsymbol{\beta}$ curves to $\boldsymbol{\beta}$ curves. Thus, the moduli space $\mathcal{M}(x_{2n-2}y_2, x_1y_1; \bar{\rho}_{23}, \bar{\sigma}_{12})$ cannot give a nontrivial differential. Domains such as $Q_2 + Q_3 + Q_4 + P_1 + P_2$ or $Q_2 + Q_3 + Q_4 + R_1 + P_2$ can be considered similarly to $Q_2 + Q_3 + Q_4$. In fact, they do not contribute to the nontrivial differential as long as the shape of the domain is topologically equivalent to $Q_2 + Q_3 + Q_4$.

There are two domains possibly giving a nontrivial differential; they are $Q_2 + Q_3 + P_1 + \cdots + P_{2n-3} + Q_4$ and $Q_2 + Q_3 + R_1 + P_2 + \cdots + R_{2n-3} + Q_4$. We will consider the domain $Q_2 + Q_3 + P_1 + \cdots + P_{2n-3} + Q_4$ first. It has three interpretations. Each of the interpretations comes from the choice of cuts made on the boundary of the domain. Cuts are allowed where the domain has $270°$ or $180°$ corners, or a point on the boundary intersecting $\boldsymbol{\alpha}$ curve. (Detailed discussions of domains and their cuts can be found in [Lipshitz et al. 2008, Chapter 6]. An interested reader may also want to see [Lipshitz et al. 2009] for more examples.) Thus, the domain $Q_2 + Q_3 + P_1 + \cdots + P_{2n-3} + Q_4$ has two points that possibly allow cuts; a point between ρ_1 and ρ_2, and a point between σ_2 and σ_3. Of course, it may not have any cuts at all. We list the moduli spaces of these interpretations as below:

- $\mathcal{M}(ay_{2n-1}, ay_1; \bar{\rho}_3, \bar{\rho}_2, \bar{\sigma}_{12})$,
- $\mathcal{M}(x_{2n-1}y_{2n-1}, x_{2n-1}y_1; \bar{\rho}_{23}, \bar{\sigma}_2, \bar{\sigma}_1)$,
- $\mathcal{M}(x_{2k-1}y_{2n-1}, x_{2k-1}y_1; \bar{\rho}_{23}, \bar{\sigma}_{12})$.

First, we will consider $\mathcal{M}(x_{2k-1}y_{2n-1}, x_{2k-1}y_1; \bar{\rho}_{23}, \bar{\sigma}_{12})$.

Lemma 3.3. *The modulo two count of the moduli space*

$$\mathcal{M}(\boldsymbol{x}_{2k-1}\boldsymbol{y}_{2n-1}, \boldsymbol{x}_{2k-1}\boldsymbol{y}_1; \bar{\rho}_{23}, \bar{\sigma}_{12})$$

is zero.

Proof. We will compute the signed number of the moduli space by considering the following $\mathcal{A}_\infty$-compatibility condition.

$$0 = m(m(\boldsymbol{x}_{2k-1}\boldsymbol{y}_{2n-1}), \bar{\rho}_2, \bar{\rho}_3, \bar{\sigma}_{12}) + m(m(\boldsymbol{x}_{2k-1}\boldsymbol{y}_{2n-1}, \bar{\rho}_2), \bar{\rho}_3, \bar{\sigma}_{12})$$
$$+ m(m(\boldsymbol{x}_{2k-1}\boldsymbol{y}_{2n-1}, \bar{\sigma}_{12}), \bar{\rho}_2, \bar{\rho}_3) + m(\boldsymbol{x}_{2k-1}\boldsymbol{y}_{2n-1}, \mu(\bar{\rho}_2, \bar{\rho}_3), \bar{\sigma}_{12})$$
$$+ m(m(\boldsymbol{x}_{2k-1}\boldsymbol{y}_{2n-1}, \bar{\rho}_2, \bar{\sigma}_{12}), \bar{\rho}_3) + m(m(\boldsymbol{x}_{2k-1}\boldsymbol{y}_{2n-1}, \bar{\rho}_2, \bar{\rho}_3, \bar{\sigma}_{12})).$$

The right-hand side of the equation above consists of six terms. The second term vanishes because $m(\boldsymbol{x}_{2k-1}\boldsymbol{y}_{2n-1}, \bar{\rho}_2)$ does not have the algebra element $\bar{\sigma}_2$ (note that domain Q_2 is adjacent to $\bar{\rho}_2$ and $\bar{\sigma}_2$). Similarly, the third term vanishes since $m(\boldsymbol{x}_{2k-1}\boldsymbol{y}_{2n-1}, \bar{\sigma}_{12})$ has $\bar{\sigma}_{12}$ as its input but lacks $\bar{\rho}_2$. The last term also vanishes because the Maslov index is not one. Replacing $\mu(\bar{\rho}_2, \bar{\rho}_3) = \bar{\rho}_{23}$ and $m(\boldsymbol{x}_{2k-1}\boldsymbol{y}_{2n-1}) = \boldsymbol{x}_{2n-2}\boldsymbol{y}_{2k} + \boldsymbol{x}_{2k}\boldsymbol{y}_{2n-2}$ (equation (2)), the above equation is reduced as follows.

$$0 = m(\boldsymbol{x}_{2n-2}\boldsymbol{y}_{2k}, \bar{\rho}_2, \bar{\rho}_3, \bar{\sigma}_{12}) + m(\boldsymbol{x}_{2k}\boldsymbol{y}_{2n-2}, \bar{\rho}_2, \bar{\rho}_3, \bar{\sigma}_{12})$$
$$+ m(\boldsymbol{x}_{2k-1}\boldsymbol{y}_{2n-1}, \bar{\rho}_{23}, \bar{\sigma}_{12}) + m(m(\boldsymbol{x}_{2k-1}\boldsymbol{y}_{2n-1}, \bar{\rho}_2, \bar{\sigma}_{12}), \bar{\rho}_3).$$

The first term on the right-hand side corresponds to the moduli space

$$\mathcal{M}(\boldsymbol{x}_{2n-2}\boldsymbol{y}_{2k}, \boldsymbol{x}_{2k-1}\boldsymbol{y}_1; \bar{\rho}_2, \bar{\rho}_3, \bar{\sigma}_{12}),$$

whose Maslov index is not one. The second vanishes because any domain containing $Q_2 + Q_3 + Q_4$ cannot have corners that contain $\boldsymbol{x}_{2k}$ and $\boldsymbol{y}_{2n-2}$. The last term also vanishes because the moduli space $\mathcal{M}(\boldsymbol{x}_{2k-1}\boldsymbol{y}_{2n-1}, \boldsymbol{a}\boldsymbol{y}_{2k}; \bar{\rho}_2, \bar{\sigma}_{12})$ has no holomorphic representative since the domain is an annulus and does not allow holomorphic involution, so $m(\boldsymbol{x}_{2k-1}\boldsymbol{y}_{2n-1}, \bar{\rho}_2, \bar{\sigma}_{12}) = 0$. Hence, we have $m(\boldsymbol{x}_{2k-1}\boldsymbol{y}_{2n-1}, \bar{\rho}_{23}, \bar{\sigma}_{12}) = 0$ and $\#\mathcal{M}(\boldsymbol{x}_{2k-1}\boldsymbol{y}_{2n-1}, \boldsymbol{x}_{2k-1}\boldsymbol{y}_1; \bar{\rho}_{23}, \bar{\sigma}_{12}) = 0$ modulo two. $\square$

The second interpretation is $\mathcal{M}(\boldsymbol{x}_{2n-1}\boldsymbol{y}_{2n-1}, \boldsymbol{x}_{2n-1}\boldsymbol{y}_1; \bar{\rho}_{23}, \bar{\sigma}_2, \bar{\sigma}_1)$. The domain is an annulus; each boundary consists of one $\boldsymbol{\alpha}$ curve segment and one $\boldsymbol{\beta}$ curve segment. The modulo two count of the moduli space can be computed by a similar computation above.

Lemma 3.4. *The modulo two count of the moduli space*

$$\mathcal{M}(\boldsymbol{x}_{2n-1}\boldsymbol{y}_{2n-1}, \boldsymbol{x}_{2n-1}\boldsymbol{y}_1; \bar{\rho}_{23}, \bar{\sigma}_2, \bar{\sigma}_1)$$

is one.

Proof. Again, we will consider the $\mathcal{A}_\infty$-compatibility relation as below:

$$
\begin{aligned}
0 = {}& m^2(\boldsymbol{x}_{2n-1}\boldsymbol{y}_{2n-1}, \bar{\rho}_2, \bar{\rho}_3, \bar{\sigma}_2, \bar{\sigma}_1) \\
= {}& m(m(\boldsymbol{x}_{2n-1}\boldsymbol{y}_{2n-1}), \bar{\rho}_2, \bar{\rho}_3, \bar{\sigma}_2, \bar{\sigma}_1) + m(\boldsymbol{x}_{2n-1}\boldsymbol{y}_{2n-1}, \mu(\bar{\rho}_2, \bar{\rho}_3), \bar{\sigma}_2, \bar{\sigma}_1) \\
& + m(m(\boldsymbol{x}_{2n-1}\boldsymbol{y}_{2n-1}, \bar{\rho}_2, \bar{\sigma}_2), \bar{\rho}_3, \bar{\sigma}_1) + m(m(\boldsymbol{x}_{2n-1}\boldsymbol{y}_{2n-1}, \bar{\rho}_2, \bar{\rho}_3), \bar{\sigma}_2, \bar{\sigma}_1) \\
& + m(m(\boldsymbol{x}_{2n-1}\boldsymbol{y}_{2n-1}, \bar{\sigma}_2, \bar{\sigma}_1), \bar{\rho}_2, \bar{\rho}_3) + m(m(\boldsymbol{x}_{2n-1}\boldsymbol{y}_{2n-1}, \bar{\rho}_2, \bar{\rho}_3, \bar{\sigma}_2), \bar{\sigma}_1) \\
& + m(m(\boldsymbol{x}_{2n-1}\boldsymbol{y}_{2n-1}, \bar{\rho}_2, \bar{\sigma}_2, \bar{\sigma}_1), \bar{\rho}_3) + m(m(\boldsymbol{x}_{2n-1}\boldsymbol{y}_{2n-1}, \bar{\rho}_2, \bar{\rho}_3, \bar{\sigma}_2, \bar{\sigma}_1)).
\end{aligned}
$$

We have $m(\boldsymbol{x}_{2n-1}\boldsymbol{y}_{2n-1}) = 0$ since there is no provincial domain connecting $\boldsymbol{x}_{2n-1}\boldsymbol{y}_{2n-1}$, so the first term on the right-hand side vanishes. The fourth term also vanishes because $m(\boldsymbol{x}_{2n-1}\boldsymbol{y}_{2n-1}, \bar{\rho}_2, \bar{\rho}_3) = 0$ (domain Q_2 is adjacent to both $\bar{\rho}_2$ and $\bar{\sigma}_2$). For the same reason, the fifth term vanishes.

In the sixth term, $m(\boldsymbol{x}_{2n-1}\boldsymbol{y}_{2n-1}, \bar{\rho}_2, \bar{\rho}_3, \bar{\sigma}_2)$ does not represent a domain with four corners. Recall that a domain that involves $\bar{\rho}_2$ and $\bar{\rho}_3$ must have $\bar{\sigma}_1$. Thus, the sixth term vanishes. Similarly, the seventh term also vanishes. We have $m(\boldsymbol{x}_{2n-1}\boldsymbol{y}_{2n-1}, \bar{\rho}_2, \bar{\rho}_3, \bar{\sigma}_2, \bar{\sigma}_1) = 0$ when considering the Maslov index.

Then the above compatibility relation is reduced to

$$
m(\boldsymbol{x}_{2n-1}\boldsymbol{y}_{2n-1}, \bar{\rho}_{23}, \bar{\sigma}_2, \bar{\sigma}_1) + m(m(\boldsymbol{x}_{2n-1}\boldsymbol{y}_{2n-1}, \bar{\rho}_2, \bar{\sigma}_2), \bar{\rho}_3, \bar{\sigma}_1) = 0
$$

The second term on the left-hand side equals $\boldsymbol{x}_{2n-1}\boldsymbol{y}_1 + \boldsymbol{x}_1\boldsymbol{y}_{2n-1}$. This implies modulo two count of the moduli spaces $\mathcal{M}(\boldsymbol{x}_{2n-1}\boldsymbol{y}_{2n-1}, \boldsymbol{x}_{2n-1}\boldsymbol{y}_1; \bar{\rho}_{23}, \bar{\sigma}_2, \bar{\sigma}_1)$ and $\mathcal{M}(\boldsymbol{x}_{2n-1}\boldsymbol{y}_{2n-1}, \boldsymbol{x}_1\boldsymbol{y}_{2n-1}; \bar{\rho}_{23}, \bar{\sigma}_2, \bar{\sigma}_1)$ equal one. $\qquad\square$

However, idempotents of the type-*DD* module prohibit a nontrivial differential from moduli spaces considered above. Explicitly,

$$
\begin{aligned}
\delta^1(\boldsymbol{x}_{2n-1}\boldsymbol{y}_{2n-1}) &= \rho_{12} \otimes \sigma_{23} \otimes \boldsymbol{x}_{2n-1}\boldsymbol{y}_1 + \cdots \\
&= \rho_{12}\iota_1 \otimes \sigma_{23} \otimes \boldsymbol{x}_{2n-1}\boldsymbol{y}_1 + \cdots \\
&= \rho_{12} \otimes \sigma_{23} \otimes \iota_1 \boldsymbol{x}_{2n-1}\boldsymbol{y}_1 + \cdots.
\end{aligned}
$$

Recall that $\iota_1 \boldsymbol{x}_{2n-1}\boldsymbol{y}_1 = 0$ since $\boldsymbol{x}_{2n-1}\boldsymbol{y}_1$ occupies $\alpha_1^{a,L}$ and the idempotent ι_1 also occupies the same α-arc.

The third interpretation is $\mathcal{M}(\boldsymbol{a}\boldsymbol{y}_{2n-1}, \boldsymbol{a}\boldsymbol{y}_1; \bar{\rho}_3, \bar{\rho}_2, \bar{\sigma}_{12})$. This is again an annulus and one of its boundaries has two $\boldsymbol{\alpha}$ curve segments and two $\boldsymbol{\beta}$ curve segments, thus it cannot give a nontrivial differential either.

Next, we will consider domain $Q_2 + Q_3 + R_1 + P_2 + \cdots + R_{2n-3} + Q_4$. Possible cuts may arise from a point between σ_2 and σ_3. The possible interpretations are

- $\mathcal{M}(\boldsymbol{x}_{2n-1}\boldsymbol{y}_{2n-1}, \boldsymbol{x}_1\boldsymbol{y}_{2n-1}; \bar{\rho}_{23}, \bar{\sigma}_2, \bar{\sigma}_1)$,

- $\mathcal{M}(\boldsymbol{x}_{2n-1}\boldsymbol{y}_{2k-1}, \boldsymbol{x}_1\boldsymbol{y}_{2k-1}; \bar{\rho}_{23}, \bar{\sigma}_{12})$.

By the above lemma, the modulo two count of the first moduli space is one, but because of idempotents, it cannot give a nontrivial contribution to the differential. The second moduli space has modulo two count zero by a similar computation in Lemma 3.3 or Lemma 3.4.

Algebra element containing ρ_{23}. Roughly speaking, the domains that possibly contribute to the algebra element ρ_{23} are obtained by adding regions to the domain $Q_1 + Q_2$ so that the resulting domain has at most four corners.

We will consider these domains by classifying them into three cases.

Case 1. We will first consider the following annular domains:

$$(3) \quad Q_1 + Q_2,$$

$$(4) \quad Q_1 + Q_2 + Q_4 + R_{2n-3} + P_{2n-3} + R_{2n-4},$$

$$(5) \quad Q_1 + Q_2 + Q_4 + \sum_{k=0}^{l} R_{2n-2k-3} + P_{2n-2k-3} + R_{2n-2k-4} + P_{2n-2k-4} + R_{2n-2l-3},$$

where $1 \leq l \leq n-2$. (Basically, these domains are obtained by adding an even number of regions to the top and bottom of $Q_1 + Q_2$.)

We will first consider the domain $Q_1 + Q_2$. The domain can be interpreted as $\mathcal{M}(a y_{2n-2}, ab; \bar{\rho}_{12}, \bar{\sigma}_2)$. Again, the modulo two count of the moduli space can be computed by using the $\mathcal{A}_\infty$-relation of $m^2(a y_{2n-2}, \bar{\rho}_1, \bar{\rho}_2, \bar{\sigma}_2)$. Recall that $m(a y_{2n-2}, \bar{\rho}_1) = x_{2n-1} y_{2n-1}$ and $m(x_{2n-1} y_{2n-1}, \bar{\rho}_2, \bar{\sigma}_2) = ab$ since the associated domains are rectangular.

$$0 = m(m(a y_{2n-2}, \bar{\rho}_1), \bar{\rho}_2, \bar{\sigma}_2) + m(a y_{2n-2}, (\bar{\rho}_1, \bar{\rho}_2), \bar{\sigma}_2)$$
$$+ m(m(a y_{2n-2}, \bar{\sigma}_2), \bar{\rho}_1, \bar{\rho}_2)$$
$$= ab + m(a y_{2n-2}, \bar{\rho}_{12}, \bar{\sigma}_2) + m(m(a y_{2n-2}, \bar{\sigma}_2), \bar{\rho}_1, \bar{\rho}_2).$$

The last term on the right-hand side equals zero because $m(a y_{2n-2}, \bar{\sigma}_2) = 0$ (domain Q_2 is adjacent to Reeb chords $\bar{\rho}_2$ and $\bar{\sigma}_2$). This implies $m(a y_{2n-2}, \bar{\rho}_{12}, \bar{\sigma}_2) = ab$, hence $\#\mathcal{M}(a y_{2n-2}, ab; \bar{\rho}_{12}, \bar{\sigma}_2) = 1$.

Remark 3.5. An annulus domain of this kind (i.e., an outside boundary consisting of both $\boldsymbol{\alpha}$ and $\boldsymbol{\beta}$ curves and an inside boundary of $\boldsymbol{\alpha}$ curve only, including a cut on the inside boundary) always admits a holomorphic representative; since we are free to choose the length of the cut starting from the point so that the annulus admits a biholomorphic involution of it, again in the sense of [Ozsváth and Szabó 2004b, Lemma 9.4].

The moduli space $\mathcal{M}(a y_{2n-2}, ab; \bar{\rho}_{12}, \bar{\sigma}_2) = \mathcal{M}(a y_{2n-2}, ab; \rho_{23}, \sigma_2)$ corresponding to $\rho_{23} \otimes \sigma_2 \otimes ab$ term occurs in $\delta^1(a y_{2n-2})$ in $\widehat{CFDD}$. However, the right-hand side is zero because of the idempotents.

Likewise, the second and third domains (see (4) and (5) on the previous page) allow the following interpretations:

- $\mathcal{M}(\boldsymbol{a}\boldsymbol{y}_{2j}, \boldsymbol{a}\boldsymbol{y}_{2j+2}; \bar{\rho}_{12}, \bar{\sigma}_2, \bar{\sigma}_1)$,
- $\mathcal{M}(\boldsymbol{a}\boldsymbol{y}_{2j}, \boldsymbol{a}\boldsymbol{y}_{2j+2}; \bar{\rho}_{12}, \bar{\sigma}_{12})$.

First, $\#\mathcal{M}(\boldsymbol{a}\boldsymbol{y}_{2j}, \boldsymbol{a}\boldsymbol{y}_{2j+2}; \bar{\rho}_{12}, \bar{\sigma}_2, \bar{\sigma}_1) = 1$ modulo two for reasons similar to those described in Remark 3.5. These contribute to the differential between generators $\boldsymbol{a}\boldsymbol{y}_{2j}$ and $\boldsymbol{a}\boldsymbol{y}_{2j+2}$ with an algebra element containing ρ_{23}, but all going to zero because of idempotents. (Similarly, $\#\mathcal{M}(\boldsymbol{a}\boldsymbol{b}, \boldsymbol{a}\boldsymbol{y}_2; \bar{\rho}_{12}, \bar{\sigma}_3, \bar{\sigma}_2, \bar{\sigma}_1) = 1$, but it does not affect the differential because of idempotents.)

Second, $\#\mathcal{M}(\boldsymbol{a}\boldsymbol{y}_{2j}, \boldsymbol{a}\boldsymbol{y}_{2j+2}; \bar{\rho}_{12}, \bar{\sigma}_{12}) = 0$ modulo two. It can be proved by considering the following $\mathcal{A}_\infty$-relation:

$$0 = m(m(\boldsymbol{a}\boldsymbol{y}_{2j}, \bar{\rho}_{12}, \bar{\sigma}_1, \bar{\sigma}_2)) + m(m(\boldsymbol{a}\boldsymbol{y}_{2j}, \bar{\sigma}_1), \bar{\rho}_{12}, \bar{\sigma}_2)$$
$$+ m(m(\boldsymbol{a}\boldsymbol{y}_{2j}, \bar{\rho}_{12}), \bar{\sigma}_1, \bar{\sigma}_2) + m(m(\boldsymbol{a}\boldsymbol{y}_{2j}, \bar{\rho}_{12}, \bar{\sigma}_1), \bar{\sigma}_2) + m(\boldsymbol{a}\boldsymbol{y}_{2j}, \bar{\rho}_{12}, (\bar{\sigma}_1, \bar{\sigma}_2)).$$

The term $m(\boldsymbol{a}\boldsymbol{y}_{2j}, \bar{\rho}_{12}, \bar{\sigma}_1, \bar{\sigma}_2) = 0$ since Maslov index is not one. We have that $m(\boldsymbol{a}\boldsymbol{y}_{2j}, \bar{\rho}_{12})$ and $m(\boldsymbol{a}\boldsymbol{y}_{2j}, \bar{\rho}_{12}, \bar{\sigma}_1)$ equal zero because $\bar{\sigma}_2$ was not involved and there is no such domain corresponding to these interpretations. From the diagram, it is clear that $m(\boldsymbol{a}\boldsymbol{y}_{2j}, \bar{\sigma}_1) = 0$. Thus, the last term $m(\boldsymbol{a}\boldsymbol{y}_{2j}, \bar{\rho}_{12}, (\bar{\sigma}_1, \bar{\sigma}_2)) = m(\boldsymbol{a}\boldsymbol{y}_{2j}, \bar{\rho}_{12}, \bar{\sigma}_{12})$ equals zero, too.

Case 2. Next, we will consider the following domains:

$$Q_1 + Q_2 + \sum_{k=0}^{l} P_{2n-2k-3} + R_{2n-2k-4} + P_{2n-2l-5},$$

$$Q_1 + Q_2 + Q_4 + \sum_{k=0}^{l} P_{2n-2k-3} + R_{2n-2k-4} + P_{2n-2l-5}$$
$$+ \sum_{k=0}^{m} R_{2n-2k-3} + P_{2n-2k-4} + R_{2n-2m-5},$$

$$Q_1 + Q_2 + Q_4 + \sum_{k=0}^{l} P_{2n-2k-3} + R_{2n-2k-4} + \sum_{k=0}^{m} R_{2n-2k-3} + P_{2n-2k-4}, \quad \text{and}$$

$$Q_1 + Q_2 + Q_4 + Q_5 + \sum_{k=0}^{n-3} P_{2n-2k-3} + R_{2n-2k-4} + \sum_{k=0}^{m} R_{2n-2k-3} + P_{2n-2k-4},$$

where $0 \le l, m \le n-3$. These domains are obtained by adding a topologically rectangular domain containing $Q_1 + Q_2$ and another rectangular domain containing Q_4.

The first domain can have a cut at a point between ρ_2 and ρ_3. The interpretation

$$\mathcal{M}(\boldsymbol{x}_{2k-1}\boldsymbol{y}_{2n-1}, \boldsymbol{x}_{2k}\boldsymbol{b}; \bar{\rho}_2, \bar{\rho}_1, \bar{\sigma}_2)$$

is essentially a rectangle so modulo two count of the corresponding moduli space is one. The second domain can have cuts at two different points; a point between

ρ_2 and ρ_3, and a point between σ_2 and σ_3. Considering the interpretation that has only one cut, the domain is an annulus with one of its boundary consisting of two $\boldsymbol{\alpha}$ curve segments and two $\boldsymbol{\beta}$ curve segments, which does not allow any holomorphic representative. If the interpretation has both of the cuts, then it is also a rectangular domain of the moduli space $\mathcal{M}(\boldsymbol{x}_{2k-1}\boldsymbol{y}_{2l-1}, \boldsymbol{x}_{2k}\boldsymbol{y}_{2l}; \bar{\rho}_2, \bar{\rho}_1, \bar{\sigma}_2, \bar{\sigma}_1)$. Dualizing them, they yield a nontrivial differential of algebra elements $\rho_{23} \otimes \sigma_2$ and $\rho_{23} \otimes \sigma_{23}$ for the type-D structure map δ^1 in $\widehat{CFDD}$.

Remark 3.6. Both of the domains considered above have interpretations without any cut. However, those interpretations do not have a holomorphic representative. For example, we can see that the modulo two count of the moduli space $\mathcal{M}(\boldsymbol{x}_{2k-1}\boldsymbol{y}_{2l-1}, \boldsymbol{x}_{2k}\boldsymbol{y}_{2l}; \bar{\rho}_{12}, \bar{\sigma}_{12})$ equals zero by considering an $\mathcal{A}_\infty$-relation similar to that discussed in Lemmas 3.3 and 3.4.

The third domain has almost the same interpretation; the only meaningful one is

$$\mathcal{M}(\boldsymbol{x}_{2l}\boldsymbol{y}_{2k}, \boldsymbol{x}_{2l+1}\boldsymbol{y}_{2k+1}; \bar{\rho}_2, \bar{\rho}_1, \bar{\sigma}_2, \bar{\sigma}_1).$$

Again, this interpretation is rectangular and modulo two count of the moduli space is one.

The last domain has two interpretations with Maslov index one. They are

$$\mathcal{M}(\boldsymbol{x}_{2l}\boldsymbol{b}, \boldsymbol{x}_{2l+1}\boldsymbol{y}_1; \bar{\rho}_2, \bar{\rho}_1, \bar{\sigma}_3, \bar{\sigma}_2, \bar{\sigma}_1)$$

and

$$\mathcal{M}(\boldsymbol{x}_{2l}\boldsymbol{b}, \boldsymbol{x}_{2l+1}\boldsymbol{y}_1; \bar{\rho}_2, \bar{\rho}_1, \bar{\sigma}_{123}).$$

The first interpretation is clearly a rectangle. However, the second one is topologically a punctured torus. To count the signed number of the moduli space, we investigate the $\mathcal{A}_\infty$-relation $m^2(\boldsymbol{x}_{2l}\boldsymbol{b}, \bar{\rho}_2, \bar{\rho}_1, \bar{\sigma}_{12}, \bar{\sigma}_3) = 0$.

Lemma 3.7. *The modulo two count of the moduli space*

$$\mathcal{M}(\boldsymbol{x}_{2l}\boldsymbol{b}, \boldsymbol{x}_{2l+1}\boldsymbol{y}_1; \bar{\rho}_2, \bar{\rho}_1, \bar{\sigma}_{123})$$

is one.

Proof. Disregarding all terms that equal zero, the relation is reduced to

$$m(\boldsymbol{x}_{2l}\boldsymbol{b}, \bar{\rho}_2, \bar{\rho}_1, \bar{\sigma}_{123}) + m(m(\boldsymbol{x}_{2l}\boldsymbol{b}, \bar{\rho}_2, \bar{\rho}_1, \bar{\sigma}_{12}), \bar{\sigma}_3) = 0.$$

$m(\boldsymbol{x}_{2l}\boldsymbol{b}, \bar{\rho}_2, \bar{\rho}_1, \bar{\sigma}_{12}) = \boldsymbol{x}_{2l+2}\boldsymbol{b}$ because the corresponding domain is an annulus as in Remark 3.5. Thus, the relation is reduced to

$$m(\boldsymbol{x}_{2l}\boldsymbol{b}, \bar{\rho}_2, \bar{\rho}_1, \bar{\sigma}_{123}) + m(\boldsymbol{x}_{2l+2}\boldsymbol{b}, \bar{\sigma}_3) = 0.$$
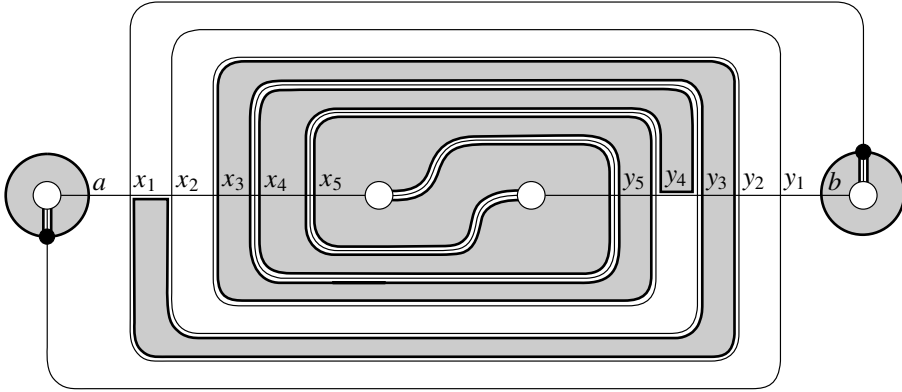
Figure 4. A diagram of the $(2, 6)$-torus link complement. The shaded region is a domain obtained by adding a rectangular domain to Q_2. This domain corresponds to a differential from $\boldsymbol{x}_1 \boldsymbol{y}_3$ to $\boldsymbol{x}_2 \boldsymbol{y}_2$. Cutting along the bold curve on the boundary of the domain, the domain turns out to be rectangular.

The second term of the right-hand side is clearly $\boldsymbol{x}_{2l+1} \boldsymbol{y}_1 + \boldsymbol{x}_1 \boldsymbol{y}_{2l+1}$. This implies modulo two count of the moduli space

$$\mathcal{M}(\boldsymbol{x}_{2l} \boldsymbol{b}, \boldsymbol{x}_{2l+1} \boldsymbol{y}_1; \bar{\rho}_2, \bar{\rho}_1, \bar{\sigma}_{123})$$

equals one.   □

Therefore, the two interpretations of the last domain result in the two same terms $\rho_{23} \otimes \sigma_{123} \otimes \boldsymbol{x}_{2l+1} \boldsymbol{y}_1$ in the $\widehat{CFDD}$ module; so they do not contribute to the differential.

Remark 3.8. Lemma 3.7 also proves that modulo two count of

$$\mathcal{M}(\boldsymbol{x}_{2l} \boldsymbol{b}, \boldsymbol{x}_1 \boldsymbol{y}_{2l+1}; \bar{\rho}_2, \bar{\rho}_1, \bar{\sigma}_{123})$$

also equals one.

<u>Case 3.</u> Domains that possibly contribute to a differential with an algebra element containing ρ_{23} are obtained by adding domains to the top of $Q_1 + Q_2$. That is, we add $2j - 1$ domains, $j = 1, \ldots, n - 1$ on the top and the resulting domain is $R_{2n-2j-1} + \cdots + R_{2n-3} + Q_1 + Q_2$. The only possible interpretation is $\mathcal{M}(\boldsymbol{x}_{2n-1} \boldsymbol{y}_{2n-2j-1}, \boldsymbol{x}_{2n-2j} \boldsymbol{b}; \bar{\rho}_{12}, \bar{\sigma}_2)$. It does not allow any holomorphic representative because the domain does not allow any holomorphic involution interchanging two boundaries.

Likewise, we shall consider domains obtained by adding domains to Q_2 on the top and bottom. Consider a domain

$$Q_1 + Q_2 + Q_4 + (R_{2n-k} + \cdots + R_{2n-3}) + (P_{2n-l} + \cdots + P_{2n-3}).$$

The domain is obtained by adding $k - 2$ domains on the top and $l - 2$ domains on the bottom of $Q_1 + Q_2 + Q_4$ (k and l should have the same parity). If $k = l$, then the resulting domain is the domain that we have considered in Case 2. (See the bottom right of Figure 5.) If $k \neq l$, then three interpretations are possible. The first is $\mathcal{M}(\boldsymbol{x}_{2n-l-2}\boldsymbol{y}_{2n-k-2}, \boldsymbol{x}_{2n-k-1}\boldsymbol{y}_{2n-l-1}; \bar{\rho}_{12}, \bar{\sigma}_{12})$. This is a genus two domain, and modulo two count of this moduli space is zero by a similar reason given in Lemma 3.3. The second and third interpretations are

$$\mathcal{M}(\boldsymbol{x}_{2n-l-2}\boldsymbol{y}_{2n-k-2}, \boldsymbol{x}_{2n-k-1}\boldsymbol{y}_{2n-l-1}; \bar{\rho}_{12}, \bar{\sigma}_2, \bar{\sigma}_1),$$

$$\mathcal{M}(\boldsymbol{x}_{2n-l-2}\boldsymbol{y}_{2n-k-2}, \boldsymbol{x}_{2n-k-1}\boldsymbol{y}_{2n-l-1}; \bar{\rho}_2, \bar{\rho}_1, \bar{\sigma}_{12}).$$

These are both annular interpretations, and they do not have any holomorphic representative because they do not allow a holomorphic involution.

Lastly, if $k = 2n - 2$, then, the domain contains Q_5. Then this domain has the two interpretations

$$\mathcal{M}(\boldsymbol{x}_{2l-2}\boldsymbol{b}, \boldsymbol{x}_1\boldsymbol{y}_{2l-1}; \bar{\rho}_2, \bar{\rho}_1, \bar{\sigma}_{123}) \quad \text{and} \quad \mathcal{M}(\boldsymbol{x}_{2l-2}\boldsymbol{b}, \boldsymbol{x}_1\boldsymbol{y}_{2l-1}; \bar{\rho}_2, \bar{\rho}_1, \bar{\sigma}_3, \bar{\sigma}_{12}).$$

The signed number of the moduli space of the first interpretation was proved to be one modulo two by Lemma 3.7. The signed number of the second interpretation is not one because it does not allow a holomorphic involution either.

To sum up, the differentials that give the algebra element containing ρ_{23} are listed below:

- $\boldsymbol{x}_i\boldsymbol{y}_j \mapsto \rho_{23} \otimes \sigma_{23} \otimes \boldsymbol{x}_{i+1}\boldsymbol{y}_{j+1}$ if $i, j \neq 2n - 1$,
- $\boldsymbol{x}_i\boldsymbol{y}_{2n-1} \mapsto \rho_{23} \otimes \sigma_2 \otimes \boldsymbol{x}_{i+1}\boldsymbol{b}$ if $j = 2n - 1$ and $i = 1, 3, \ldots, 2n - 3$,
- $\boldsymbol{x}_i\boldsymbol{b} \mapsto \rho_{23} \otimes \sigma_{123} \otimes \boldsymbol{x}_1\boldsymbol{y}_{i+1}$.

Algebra element contains ρ_{123}. Domains that possibly contribute to the algebra element ρ_{123} are listed below:

$$(Q_1 + Q_2 + Q_3 + Q_4) + (R_1 + P_2 + R_3 + P_4 + \cdots + R_{2n-5} + P_{2n-4}) + R_{2n-3};$$

$$(Q_1 + Q_2 + Q_3 + Q_4) + (P_1 + \cdots + P_{2n-3});$$

$$(Q_1 + Q_2 + Q_3 + Q_4) + \sum_{k=0}^{l}(R_{2k+1} + P_{2k+2})$$
$$+ \sum_{k=0}^{n-4-l}(R_{2n-2k-3} + P_{2n-2k-3} + R_{2n-2k-4} + P_{2n-2k-4}) + R_{2l+3};$$

$$(Q_1 + Q_2 + Q_3 + Q_4) + \sum_{k=0}^{l}(P_{2k+1} + P_{2k+2})$$
$$+ \sum_{k=0}^{n-4-l}(R_{2n-2k-3} + P_{2n-2k-3} + R_{2n-2k-4} + P_{2n-2k-4}) + P_{2l+3}; \quad \text{and}$$

$$Q_1 + \cdots + Q_5 + P_1 + \cdots + P_{2n-3} + R_1 + \cdots + R_{2n-3},$$
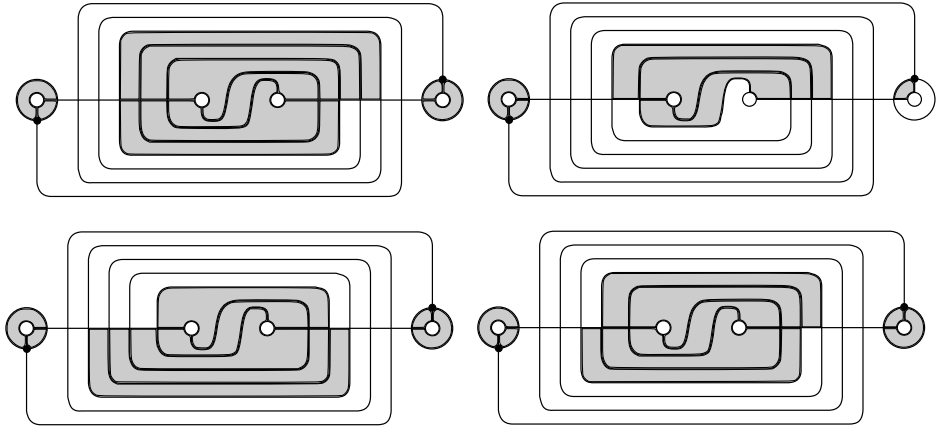
Figure 5. Examples of obtaining nonrectangular domains of the $(2, 6)$-torus link. Top left can be interpreted as an annular domain, but it cannot give a nontrivial differential due to idempotents. Top right is obtained by adding a domain to Q_2 on the top, but its only possible interpretation does not allow any holomorphic representative. Bottom left and bottom right are obtained by adding domains to Q_2 on the top and bottom. If the number of regions attached on the top is not equal to the number of regions attached on the bottom, it has two interpretations; and they do not allow a holomorphic representative either (bottom left). If two numbers are equal, then the domain gives a nontrivial differential. (This case was previously considered. See Figure 4.)

where $1 \leq l \leq n - 3$.

Each of these domains are obtained by adding a rectangular domain containing a region adjacent to ρ_1 to the annular domain listed in the algebra element containing ρ_{23}.

We investigate the first domain. As before, we list all possible interpretations:

- $\mathcal{M}(\boldsymbol{a}\boldsymbol{y}_{2n-2}, \boldsymbol{x}_1\boldsymbol{y}_{2n-1}; \bar{\rho}_{123}, \bar{\sigma}_2, \bar{\sigma}_1)$,

- $\mathcal{M}(\boldsymbol{a}\boldsymbol{y}_{2n-2}, \boldsymbol{x}_1\boldsymbol{y}_{2n-1}; \bar{\rho}_3, \bar{\rho}_2, \bar{\rho}_1, \bar{\sigma}_2, \bar{\sigma}_1)$,

- $\mathcal{M}(\boldsymbol{a}\boldsymbol{y}_{2n-2}, \boldsymbol{x}_1\boldsymbol{y}_{2n-1}; \bar{\rho}_{23}, \bar{\rho}_1, \bar{\sigma}_2, \bar{\sigma}_1)$,

- $\mathcal{M}(\boldsymbol{a}\boldsymbol{y}_{2n-2}, \boldsymbol{x}_1\boldsymbol{y}_{2n-1}; \bar{\rho}_3, \bar{\rho}_{12}, \bar{\sigma}_2, \bar{\sigma}_1)$.

The third interpretation is an annulus whose outer boundary has two $\boldsymbol{\alpha}$ curve segments and two $\boldsymbol{\beta}$ curve segments; thus it does not have a holomorphic representative. The fourth interpretation cannot give a nontrivial contribution either because of the $\mathcal{A}_\infty$-module compatibility relation. On the other hand, the second interpretation is

a rectangular one; it allows a holomorphic representative and its modulo two count of the moduli space is one. The first interpretation also has a moduli space with modulo two count one by the same analysis in Lemma 3.7. Again, the first and second interpretations will result in the same term after in $\widehat{CFDD}$ module. The sum of these two terms equals zero, so this domain actually has no contribution after all.

The second domain has two interpretations; $\mathcal{M}(\boldsymbol{a}\boldsymbol{y}_{2n-2}, \boldsymbol{x}_{2n-1}\boldsymbol{y}_1; \bar{\rho}_{123}, \bar{\sigma}_2, \bar{\sigma}_1)$ and $\mathcal{M}(\boldsymbol{a}\boldsymbol{y}_{2n-2}, \boldsymbol{x}_{2n-1}\boldsymbol{y}_1; \bar{\rho}_3, \bar{\rho}_{12}, \bar{\sigma}_2, \bar{\sigma}_1)$. The first interpretation was considered in the above computation, and the second interpretation is an annulus whose outer boundary consists of two $\boldsymbol{\alpha}$ curve segments and two $\boldsymbol{\beta}$ curve segments, so there is no holomorphic representative.

Similarly, the other domains (except for the last) give Whitney disks, and the moduli spaces corresponding to the domains are $\mathcal{M}(\boldsymbol{a}\boldsymbol{y}_{2j}, \boldsymbol{x}_1\boldsymbol{y}_{2j+1}; \bar{\rho}_{123}, \bar{\sigma}_2, \bar{\sigma}_1)$, $\mathcal{M}(\boldsymbol{a}\boldsymbol{y}_{2j}, \boldsymbol{x}_1\boldsymbol{y}_{2j+1}; \bar{\rho}_3, \bar{\rho}_2, \bar{\rho}_1, \bar{\sigma}_2, \bar{\sigma}_1)$ and $\mathcal{M}(\boldsymbol{a}\boldsymbol{y}_{2j}, \boldsymbol{x}_{2j+1}\boldsymbol{y}_1; \bar{\rho}_{123}, \bar{\sigma}_2, \bar{\sigma}_1)$. The signed number of each of these moduli spaces is one modulo two.

The moduli space of the last domain $Q_1 + \cdots + Q_5 + P_1 + \cdots + P_{2n-3} + Q_1 + \cdots + Q_{2n-3}$ can be interpreted in four ways. The first is $\mathcal{M}(\boldsymbol{a}\boldsymbol{b}, \boldsymbol{x}_1\boldsymbol{y}_1; \bar{\rho}_{123}, \bar{\sigma}_{123})$ whose Maslov index is different from one. The second possible interpretation is

$$\mathcal{M}(\boldsymbol{a}\boldsymbol{b}, \boldsymbol{x}_1\boldsymbol{y}_1; \bar{\rho}_{123}, \bar{\sigma}_3, \bar{\sigma}_2, \bar{\sigma}_1)$$

$\mathcal{A}_\infty$-relation of $m^2(\boldsymbol{a}\boldsymbol{b}, \bar{\rho}_{12}, \bar{\rho}_3, \bar{\sigma}_3, \bar{\sigma}_2, \bar{\sigma}_1)$ gives $m(\boldsymbol{a}\boldsymbol{b}, \bar{\rho}_{123}, \bar{\sigma}_3, \bar{\sigma}_2, \bar{\sigma}_1) = \boldsymbol{x}_1\boldsymbol{y}_1$, by considering $m(\boldsymbol{a}\boldsymbol{b}, \bar{\rho}_{12}, \bar{\sigma}_3, \bar{\sigma}_2, \bar{\sigma}_1) = \boldsymbol{a}\boldsymbol{y}_2$ and $m(\boldsymbol{a}\boldsymbol{y}_2, \bar{\rho}_3) = \boldsymbol{x}_1\boldsymbol{y}_1$. Thus, the modulo two count of the moduli space is one. The third interpretation

$$\mathcal{M}(\boldsymbol{a}\boldsymbol{b}, \boldsymbol{x}_1\boldsymbol{y}_1; \bar{\rho}_3, \bar{\rho}_2, \bar{\rho}_1, \bar{\sigma}_{123})$$

can be done precisely in the same way. The last interpretation is

$$\mathcal{M}(\boldsymbol{a}\boldsymbol{b}, \boldsymbol{x}_1\boldsymbol{y}_1; \bar{\rho}_3, \bar{\rho}_2, \bar{\rho}_1, \bar{\sigma}_3, \bar{\sigma}_2, \bar{\sigma}_1)$$

The existence of a holomorphic curve and its modulo two count is quite clear from the diagram; the domain is essentially rectangular in this interpretation.

It is worth mentioning that there are three moduli spaces contributing to $\rho_{123}\sigma_{123} \otimes \boldsymbol{x}_1\boldsymbol{y}_1$ term in $\delta^1(\boldsymbol{a}\boldsymbol{b})$.

To sum up, we have the following nontrivial differentials of the algebra element containing ρ_{123}:

- $\boldsymbol{a}\boldsymbol{y}_{2k} \mapsto \rho_{123} \otimes \sigma_{23} \otimes \boldsymbol{x}_{2k+1}\boldsymbol{y}_1$,

- $\boldsymbol{a}\boldsymbol{b} \mapsto \rho_{123} \otimes \sigma_{123} \otimes \boldsymbol{x}_1\boldsymbol{y}_1$.

For the algebra elements containing σ_{12}, σ_{23} and σ_{123}, those differentials can be computed in a parallel manner by taking advantage of the symmetry of the diagram.

We close this section by summarizing the computation:

Proposition 3.9. *Let $\mathcal{H}$ be a bordered Heegaard diagram of $(2, 2n)$-torus link complement in S^3 as in Figure 2. Then, $\widehat{CFDD}(\mathcal{H})$ has the following generators*:

- $x_i y_j$, *where $1 \le i, j \le 2n - 1$ and $i = j$ modulo two,*

- ab,

- $a y_k$, *where $k = 2, 4, \ldots, 2n - 2$,*

- $x_k b$, *where $k = 2, 4, \ldots, 2n - 2$.*

The map $\delta^1 : \mathfrak{S}(\mathcal{H}) \to \mathcal{A}(-\mathcal{Z}_L) \otimes \mathcal{A}(-\mathcal{Z}_R) \otimes \mathfrak{S}(\mathcal{H})$ is computed in the following way.

- *For $x_i y_j$, if $i, j \ne 2n - 1$,*

$$
x_i y_j \mapsto \begin{cases}
x_{j-1} y_{i+1} + x_{i+1} y_{j-1} + \rho_{23}\sigma_{23} x_{i+1} y_{j+1} & \text{if } j - i > 2, \\
x_{j+1} y_{i-1} + x_{i-1} y_{j+1} + \rho_{23}\sigma_{23} x_{i+1} y_{j+1} & \text{if } i - j > 2, \\
x_{i+1} y_{j-1} + \rho_{23}\sigma_{23} x_{i+1} y_{j+1} & \text{if } j - i = 2, \\
x_{i-1} y_{j+1} + \rho_{23}\sigma_{23} x_{i+1} y_{j+1} & \text{if } i - j = 2, \\
\rho_{23}\sigma_{23} x_{i+1} y_{j+1} & \text{if } i = j.
\end{cases}
$$

- *If $j = 2n - 1$ and $i = 1, 3, \ldots, 2n - 3$,*

$$
x_i y_j \mapsto \begin{cases}
x_{j-1} y_{i+1} + x_{i+1} y_{j-1} + \rho_{23}\sigma_2 x_{i+1} b & \text{if } j - i > 2, \\
x_{i+1} y_{j-1} + \rho_{23}\sigma_2 x_{i+1} b & \text{if } i = 2n - 3.
\end{cases}
$$

- *If $i = 2n - 1$ and $j = 1, 3, \ldots, 2n - 3$,*

$$
x_i y_j \mapsto \begin{cases}
x_{j+1} y_{i-1} + x_{i-1} y_{j+1} + \rho_2 \sigma_{23} a y_{j+1} & \text{if } i - j > 2, \\
x_{j+1} y_{i-1} + \rho_2 \sigma_{23} a y_{j+1} & \text{if } j = 2n - 3.
\end{cases}
$$

- $x_{2n-1} y_{2n-1} \mapsto \rho_2 \sigma_2 ab$.

- $a y_j \mapsto$

$$
\begin{cases}
\rho_1 x_1 y_1 + \rho_3(x_{2n-1} y_3 + x_3 y_{2n-1}) + \rho_{123}\sigma_{23} x_3 y_1 & \text{if } j = 2, \\
\rho_1(x_1 y_{2n-3} + x_{2n-3} y_1) + \rho_3 x_{2n-1} y_{2n-1} + \rho_{123}\sigma_{23} x_{2n-1} y_1 & \text{if } j = 2n - 2, \\
\rho_1(x_1 y_{j-1} + x_{j-1} y_1) + \rho_3(x_{2n-1} y_{j+1} + x_{j+1} y_{2n-1}) + \rho_{123}\sigma_{23} x_{j+1} y_1 & \\
& \text{otherwise.}
\end{cases}
$$

- $x_i b \mapsto$

$$
\begin{cases}
\sigma_1 x_1 y_1 + \sigma_3(x_3 y_{2n-1} + x_{2n-1} y_3) + \rho_{23}\sigma_{123} x_1 y_3 & \text{if } i = 2, \\
\sigma_1(x_{2n-3} y_1 + x_1 y_{2n-3}) + \sigma_3 x_{2n-1} y_{2n-1} + \rho_{23}\sigma_{123} x_1 y_{2n-1} & \text{if } i = 2n - 2, \\
\sigma_1(x_{i-1} y_1 + x_1 y_{i-1}) + \sigma_3(x_{i+1} y_{2n-1} + x_{2n-1} y_{i+1}) + \rho_{23}\sigma_{123} x_1 y_{i+1} & \\
& \text{otherwise.}
\end{cases}
$$

- $ab \mapsto (\rho_1 \sigma_3 + \rho_3 \sigma_1)(x_1 y_{2n-1} + x_{2n-1} y_1) + \rho_{123}\sigma_{123} x_1 y_1$.

Figure 6. A diagram of the $(2, 6)$-torus link complement. The arrows emanating from a generator in the box show the resulting terms of the differential of the generator. The dashed arrow represents algebra element $\rho_{23}\sigma_{123}$, the dotted arrow $\rho_{123}\sigma_{23}$, and the doubly dashed arrow $\rho_{23}\sigma_{23}$. Other algebra elements are written on the arrows.

4. Examples

In this section, we will relate our result to the known calculation for knot complements and closed 3-manifolds. These examples show how to use the algebraic structure of the pairing theorem given in [Lipshitz et al. 2008].

Derived tensor product of bimodule. The pairing of modules associated to a single boundary three-manifold is well studied in [Lipshitz et al. 2008]. In this section, we will be using the pairing theorem of doubly bordered cases. There are many versions of the pairing theorem depending on the types of bimodules [Lipshitz et al. 2015, Theorem 2], but for our purpose, the pairing of a type-A module and type-DD module will suffice.

The pairing of bimodules associated to double bordered three-manifold is also similar to the single boundary case; the only difference is the framed arc z. If we glue a doubly bordered diagram and a single boundary diagram together, we match the marked point z from the single boundary diagram with one end of the framed arc z. After pairing, the framed arc is reduced to a marked point on the other side of the boundary (when pairing two doubly bordered diagrams, then we connect the two framed arcs). In our example, we will be mainly interested in a type-D structure obtained by the derived tensor product $\widehat{CFA}(\mathcal{H}_1)\widetilde{\otimes}_{\mathcal{A}(\mathcal{Z})}\widehat{CFDD}(\mathcal{H}_2)$, where a single boundary diagram $\mathcal{H}_1$ is glued on the right side of a doubly bordered diagram $\mathcal{H}_2$. The resulting type-D structure map $(\delta')^1$ is

$$(\delta')^1 = \sum_{k=1}^{\infty}((m_R)_{k+1}\otimes\mu_L\otimes\mathbb{I}_{\widehat{CFDD}})(\boldsymbol{x}\otimes\delta^k(\boldsymbol{y}))$$

where $\boldsymbol{x}\in\mathfrak{S}(\mathcal{H}_1)$ and $\boldsymbol{y}\in\mathfrak{S}(\mathcal{H}_2)$.

Infinity-surgery on right component of link. First, we will consider an ∞-surgery on the right component of the $(2,2n)$-torus link complement. Since the longitudes $\alpha_1^{a,L}$ and $\alpha_1^{a,R}$ of the left and right components are passing through β_1 and β_2 respectively, the ∞-surgery on the right components gives an unknot complement with framing $(n-1)$. We compute $\widehat{CFD}$ of the unknot complement as follows.

Let $\mathcal{H}_{(2,2n)}$ be a doubly bordered diagram of the $(2,2n)$-torus link complement, and $\mathcal{H}_\infty$ be a single bordered diagram of a solid torus with ∞-framing. Then, the generator set $\mathfrak{S}(\mathcal{H}_\infty\cup_\partial\mathcal{H}_{(2,2n)})$ consists of $\boldsymbol{w}\otimes\boldsymbol{ab}$ and $\boldsymbol{w}\otimes x_{2k}\boldsymbol{b}$, $k=1,\ldots,n-1$.

Computing $\widehat{CFA}(\mathcal{H}_\infty)$ is easy; that is,

$$m_{k+3}(\boldsymbol{w},\sigma_3,\underbrace{\sigma_{23},\ldots,\sigma_{23}}_{k\text{-times}},\sigma_2)=\boldsymbol{w}.$$

Now, we shall consider the type-D structure of $\widehat{CFDD}(\mathcal{H}_{(2,2n)})$. We omit the terms which do not appear after taking box tensor product with $\widehat{CFA}(\mathcal{H}_\infty)$; thus, they have no contribution in computing $\widehat{CFA}(\mathcal{H}_\infty)\widetilde{\otimes}_{\mathcal{A}(\mathcal{Z})}\widehat{CFDD}(\mathcal{H}_{(2,2n)})$.

$$\delta^2(\boldsymbol{ab})=(\rho_1\otimes\rho_{23})\otimes(\sigma_3\otimes\sigma_2)\otimes x_2\boldsymbol{b}+\cdots,$$
$$\delta^2(x_{2k}\boldsymbol{b})=(\rho_{23})\otimes(\sigma_3\otimes\sigma_2)\otimes x_{2k+2}\boldsymbol{b}+\cdots\qquad\text{for }k=1,\ldots,n-2,$$
$$\delta^2(x_{2n-2}\boldsymbol{b})=(\rho_2)\otimes(\sigma_3\otimes\sigma_2)\otimes\boldsymbol{ab}+\cdots.$$

Thus, the type-D structure $(\delta')^1$ is

$$(\delta')^1(\boldsymbol{w} \otimes \boldsymbol{ab}) = \mu(\rho_1 \otimes \rho_{23}) \otimes m_3(\boldsymbol{w}, \sigma_3, \sigma_2) \otimes \boldsymbol{x}_2\boldsymbol{b} = \rho_{123} \otimes \boldsymbol{w} \otimes \boldsymbol{x}_2\boldsymbol{b},$$
$$(\delta')^1(\boldsymbol{w} \otimes \boldsymbol{x}_{2k}\boldsymbol{b}) = \mu(\rho_{23}) \otimes m_3(\boldsymbol{w}, \sigma_3, \sigma_2) \otimes \boldsymbol{x}_{2k+2}\boldsymbol{b} = \rho_{23} \otimes \boldsymbol{w} \otimes \boldsymbol{x}_{2k+2}\boldsymbol{b}$$

$$\text{for } k = 1, \ldots, n-2,$$

$$(\delta')^1(\boldsymbol{w} \otimes \boldsymbol{x}_{2n-2}\boldsymbol{b}) = \mu(\rho_2) \otimes m_3(\boldsymbol{w}, \sigma_3, \sigma_2) \otimes \boldsymbol{ab} = \rho_2 \otimes \boldsymbol{w} \otimes \boldsymbol{ab}.$$

Compare this result with [Hom 2011, Example 2.2].

Knot complement of trefoil. Consider the $(2, 4)$-torus link complement. If we glue the right component with a solid torus of framing $+2$, then the resulting manifold will be diffeomorphic to a trefoil complement (after handleslide and blowing down the $+1$ unknot component). A type-D structure

$$(N_1, (\delta_1)^1) := \widehat{CFA}(\mathcal{H}_{+2}) \widetilde{\otimes}_{\mathcal{A}(\mathcal{Z})} \widehat{CFDD}(\mathcal{H}_{(2,4)})$$

computes as
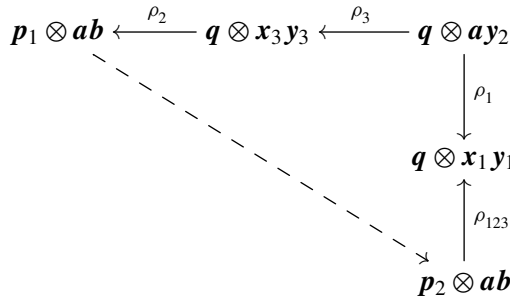
The dashed line is called an *unstable chain*, where

We claim that the chain complex described above is homotopy equivalent to a complex $(N_2, (\delta_2)^1)$, which is identical to the complex above except for the unstable complex that has been replaced by

$$\cdots \to \boldsymbol{p}_1 \otimes \boldsymbol{ab} \xrightarrow{\rho_{123}} \boldsymbol{p}_2 \otimes \boldsymbol{x}_2\boldsymbol{b} \xrightarrow{\rho_{23}} \boldsymbol{q} \otimes \boldsymbol{x}_1\boldsymbol{y}_3 \xrightarrow{\rho_{23}} \boldsymbol{p}_1 \otimes \boldsymbol{x}_2\boldsymbol{b} \xrightarrow{\rho_2} \boldsymbol{p}_2 \otimes \boldsymbol{ab} \to \cdots$$

Define a map $\pi : N_1 \to N_2$ such that $\pi(\boldsymbol{q} \otimes \boldsymbol{x}_3\boldsymbol{y}_1) = 0$, $\pi(\boldsymbol{q} \otimes \boldsymbol{x}_2\boldsymbol{y}_2) = 0$, and otherwise identity. We also define a map $\iota : N_2 \to N_1$ as an inclusion. Then, $\pi \circ \iota = \mathbb{I}_{N_2}$ is obvious. In addition, a homotopy equivalence $H : N_1 \to N_1$ is given

as

$$H(x) := \begin{cases} \boldsymbol{q} \otimes \boldsymbol{x}_3 \boldsymbol{y}_1 & \text{if } x = \boldsymbol{q} \otimes \boldsymbol{x}_2 \boldsymbol{y}_2, \\ \boldsymbol{q} \otimes \boldsymbol{x}_1 \boldsymbol{y}_3 + \boldsymbol{q} \otimes \boldsymbol{x}_3 \boldsymbol{y}_1 & \text{if } x = \boldsymbol{q} \otimes \boldsymbol{x}_1 \boldsymbol{y}_3, \\ \boldsymbol{p}_2 \otimes \boldsymbol{x}_2 \boldsymbol{b} & \text{if } x = \boldsymbol{p}_2 \otimes \boldsymbol{x}_2 \boldsymbol{b}, \\ 0 & \text{otherwise,} \end{cases}$$

which extends to a $\mathcal{A}(T)$-equivariant map. It is clear that $\iota \circ \pi = (\delta_1)^1 \circ H + H \circ (\delta_1)^1$.

Remark 4.1. Compare this result with [Lipshitz et al. 2008, Section 11.5], from which they spelled out an algorithm to recover $\widehat{CFD}(S^3 \backslash \nu K)$ from CFK^-. According to their notation, the length of the unstable chain is 3 (the number of generators between two outermost ones). This length is closely related to the framing of the knot complement and concordance invariant $\tau(K)$; see [Lipshitz et al. 2008, equation (11.18)]. In our case, the framing of the left component of the link was originally -1, but a handleslide procedure has added +4 and therefore the framing is 3. Since $\tau(\text{Trefoil}) = 1$ is less than the framing, the length of the unstable chain agrees with the framing. Interested readers will find the precise description of the relation between $\tau(K)$ and the unstable chain in [Lipshitz et al. 2008, Theorem A.11].

An integral surgery on Hopf link. Hopf link is $(2, 2)$-torus link. If n_1 and n_2 are two positive integers such that $n_1 n_2 \neq 1$, then (n_1, n_2)-surgery on Hopf link produces the lens space $L(n_1 n_2 - 1, n_1)$. The Heegaard Floer homology of the lens space has $n_1 n_2 - 1$ generators whose differentials equal zero.

The diagram of the Hopf link complement is easy. In addition, $\alpha_1^{a,L}$ and $\alpha_1^{a,R}$ do not intersect β_1 and β_2, respectively; therefore pairing the diagram with $\mathcal{H}_{n_1}^L$ and $\mathcal{H}_{n_2}^R$ will give a closed Heegaard diagram of the lens space $L(n_1 n_2 - 1, n_1)$. The $\mathcal{A}_\infty$-relation of $\widehat{CFA}(\mathcal{H}_m)$ is as follows (see Figure 7):

$$m(q, \rho_2) = p_1,$$

$$m(p_i, \rho_3, \underbrace{\rho_{23}, \dots, \rho_{23}}_{j \text{ times}}, \rho_2) = p_{i+j+1},$$

$$m(p_m, \rho_3, \rho_2, \rho_1) = q.$$

$\widehat{CFDD}(S^3 \backslash \nu(\text{Hopf link}))$ has two generators $\boldsymbol{ab}$ and $\boldsymbol{x}_1 \boldsymbol{y}_1$. Its type-$D$ structure is given below:

$$\delta^1(\boldsymbol{ab}) = (\rho_1 \otimes \sigma_3 + \rho_3 \otimes \sigma_1 + \rho_{123} \otimes \sigma_{123}) \otimes \boldsymbol{x}_1 \boldsymbol{y}_1,$$

$$\delta^1(\boldsymbol{x}_1 \boldsymbol{y}_1) = \rho_2 \otimes \sigma_2 \otimes \boldsymbol{ab}.$$

Remark 4.2. See [Lipshitz et al. 2015, Proposition 10.1]. Note that Hopf link complement is $T^2 \times [0, 1]$ and it is exactly an identity module described there.
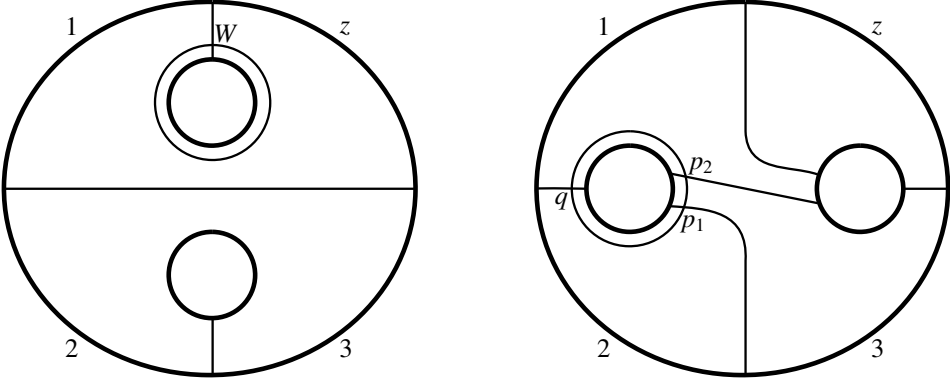
Figure 7. The diagram $\mathcal{H}_\infty$ on the left shows ∞-surgery on the right component of the link. The diagram $\mathcal{H}_{+2}$ on the right is $+2$-surgery on the right component. The $\mathcal{A}_\infty$-relation of $\widehat{CFA}(\mathcal{H}_{+2})$ is given as $m(q, \sigma_2) = p_1$, $m(p_1, \sigma_3, \sigma_2) = p_2$, and $m(p_2, \sigma_3, \sigma_2, \sigma_1) = q$.

Let p_i^L and q^L (p_j^R and q^R, respectively) be the generators of the bordered Heegaard diagram $\mathcal{H}_{n_1}^L$ attached to the left ($\mathcal{H}_{n_2}^R$ attached to the right, respectively). Then, $\widehat{CFA}(\mathcal{H}_{n_1}^L) \widetilde{\otimes}_{\mathcal{A}(\mathcal{Z})} \widehat{CFA}(\mathcal{H}_{n_2}^R) \widetilde{\otimes}_{\mathcal{A}(\mathcal{Z})} \widehat{CFDD}(S^3 \setminus \nu(\text{Hopf link}))$ has the following $n_1 n_2 + 1$ generators:

$$p_i^L \otimes p_j^R \otimes \boldsymbol{ab}, \quad i = 1, \ldots, n_1 \text{ and } j = 1, \ldots, n_2,$$
$$q^L \otimes q^R \otimes \boldsymbol{x_1 y_1}.$$

The only nontrivial differential is

$$\partial(q^L \otimes q^R \otimes \boldsymbol{x_1 y_1}) = m(q^L, \rho_2) \otimes m(q^R, \sigma_2) \otimes \boldsymbol{ab} = p_1^L \otimes p_1^R \otimes \boldsymbol{ab}.$$

Thus, the homology of $\widehat{CFA}(\mathcal{H}_{n_1}^L) \widetilde{\otimes}_{\mathcal{A}(\mathcal{Z})} \widehat{CFA}(\mathcal{H}_{n_2}^R) \widetilde{\otimes}_{\mathcal{A}(\mathcal{Z})} \widehat{CFDD}(S^3 \setminus \nu(\text{Hopf link}))$ has $n_1 n_2 - 1$ generators as expected.

5. Homotopy equivalence

In this section, we streamline the type-*DD* structure computed in Section 3 to a type-*DD* structure that does not involve any differential with the algebra element 1.

Proposition 5.1. *The type-DD structure of the link complement of the $(2, 2n)$-torus link complement, where $n \geq 3$, has the same homotopy type as the complex given in Figure 8.*

Proof. Let (M, δ^1) denote the type-*DD* structure computed in Proposition 3.9 and $(N, (\delta^1)')$ the type-*DD* structure given as Figure 8. More specifically, the map $(\delta^1)'$
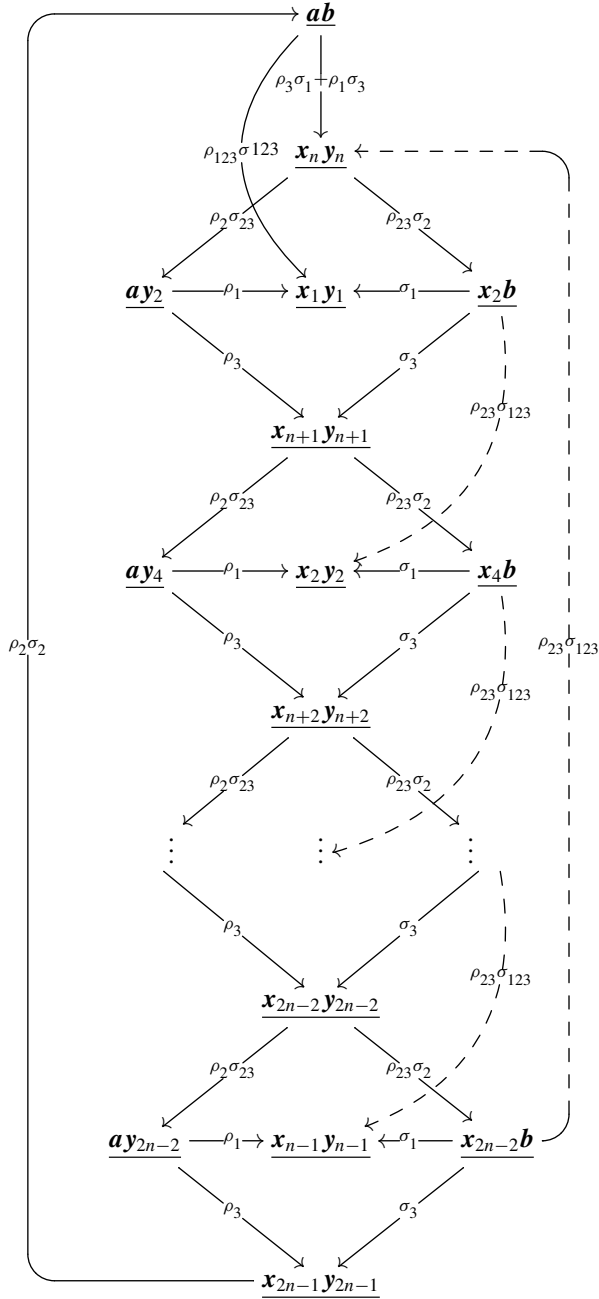
Figure 8. Simplified diagram of $\widehat{CFDD}$ of the $(2, 2n)$-torus link complement, $n \geq 3$. Note that the dashed arrows can be changed to the arrows in Figure 9.
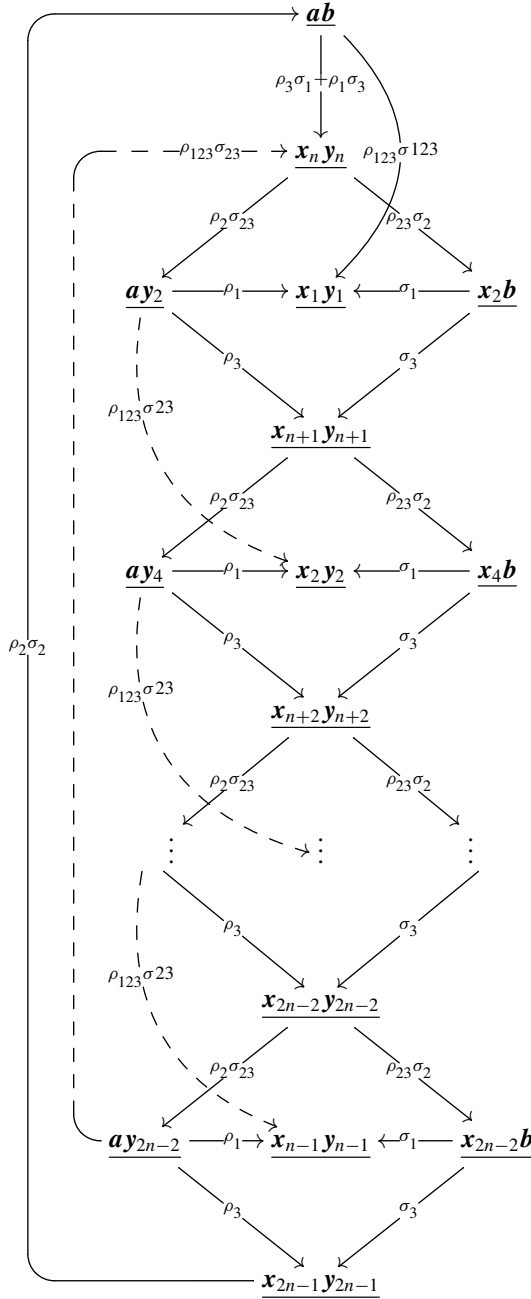
Figure 9. Another type-*DD* structure homotopy equivalent to the original type-*DD* structure. The differential represented by the dashed line can be changed to the differential in Figure 8, too.

has the following differentials:

$$\underline{ab} \mapsto \rho_{123}\sigma_{123} \otimes \underline{x_1 y_1} + (\rho_1\sigma_3 + \rho_3\sigma_1) \otimes \underline{x_n y_n},$$

$$\underline{a y_{2k}} \mapsto \rho_1 \otimes \underline{x_k y_k} + \rho_3 \otimes \underline{x_{n+k} y_{n+k}} \qquad \text{if } k = 1, \dots, n-1,$$

$$\underline{x_{2k} b} \mapsto \sigma_1 \otimes \underline{x_k y_k} + \sigma_3 \otimes \underline{x_{n+k} y_{n+k}} + \rho_{23}\sigma_{123} \otimes \underline{x_{k+1} y_{k+1}} \quad \text{if } k = 1, \dots, n-1,$$

$$\underline{x_k y_k} \mapsto 0 \qquad \text{if } k = 1, \dots, n-1,$$

$$\underline{x_k y_k} \mapsto \rho_2\sigma_{23} \otimes \underline{a y_{2(k-n+1)}} + \rho_{23}\sigma_2 \otimes \underline{x_{2(k-n+1)} b} \qquad \text{if } k = n, \dots, 2n-2,$$

$$\underline{x_{2n-1} y_{2n-1}} \mapsto \rho_2\sigma_2 \otimes \underline{ab}.$$

We shall now define type-DD structure maps $F : M \to \mathcal{A}(-\mathcal{Z}_L) \otimes \mathcal{A}(-\mathcal{Z}_R) \otimes N$ and $G : N \to \mathcal{A}(-\mathcal{Z}_L) \otimes \mathcal{A}(-\mathcal{Z}_R) \otimes M$. First, the map F is defined as below.

$$F(\boldsymbol{ab}) = \underline{ab},$$

$$F(\boldsymbol{a y_{2k}}) = \underline{a y_{2k}},$$

$$F(\boldsymbol{x_{2k} b}) = \underline{x_{2k} b},$$

$$F(\boldsymbol{x_1 y_{2k-1}}) = \underline{x_k y_k} \quad \text{for } k = 1, \dots, n,$$

$$F(\boldsymbol{x_{2k-1} y_{2n-1}}) = \underline{x_{k+n-1} y_{k+n-1}} \quad \text{for } k = 1, \dots, n,$$

$$F(\boldsymbol{x_{2k} y_{2n-2}}) = \rho_2\sigma_{23} \otimes \underline{a y_{2k}} \quad \text{for } k = 1, \dots, n-1,$$

and zero otherwise.

The map G is defined as follows:

$$G(\underline{ab}) = \boldsymbol{ab},$$

$$G(\underline{a y_{2k}}) = \boldsymbol{a y_{2k}},$$

$$G(\underline{x_{2k} b}) = \boldsymbol{x_{2k} b},$$

$$G(\underline{x_1 y_1}) = \boldsymbol{x_1 y_1} + \rho_{23}\sigma_{23} \otimes \boldsymbol{x_3 y_1},$$

$$G(\underline{x_k y_k}) = \boldsymbol{x_1 y_{2k-1}} + \boldsymbol{x_{2k-1} y_1} + \rho_{23}\sigma_{23} \otimes \boldsymbol{x_{2k+1} y_1} \quad \text{for } k = 2, \dots, n-1,$$

$$G(\underline{x_k y_k}) = \boldsymbol{x_{2k-2n+1} y_{2n-1}} + \boldsymbol{x_{2n-1} y_{2k-2n+1}} \quad \text{for } k = n, \dots, 2n-2,$$

$$G(\underline{x_{2n-1} y_{2n-1}}) = \boldsymbol{x_{2n-1} y_{2n-1}}.$$

These maps are easily seen satisfying the compatibility condition spelled out in [Lipshitz et al. 2015, Definition 2.2.55]. Then, the composition of two maps $F \circ G : N \to N$ is the identity map. Another composition $G \circ F$ is homotopic to identity by introducing the seemingly complicated map $H : M \to \mathcal{A}(-\mathcal{Z}_L) \otimes \mathcal{A}(-\mathcal{Z}_R) \otimes M$. For the generators of M listed below, the map H is defined as

$$H(\boldsymbol{ab}) = 0,$$

$$H(\boldsymbol{a y_{2k}}) = \rho_3 \otimes (\boldsymbol{x_{2k+1} y_{2n-1}} + \boldsymbol{x_{2n-1} y_{2k+1}}) \quad \text{for } k = 1, \dots, n-2,$$

$$H(\boldsymbol{a}\boldsymbol{y}_{2n-2}) = \rho_3 \otimes \boldsymbol{x}_{2n-1}\boldsymbol{y}_{2n-1},$$
$$H(\boldsymbol{x}_{2k}\boldsymbol{b}) = \sigma_3 \otimes (\boldsymbol{x}_{2n-1}\boldsymbol{y}_{2k+1} + \boldsymbol{x}_{2k+1}\boldsymbol{y}_{2n-1}) \quad \text{for } k = 1, \ldots, n-2,$$
$$H(\boldsymbol{x}_{2n-2}\boldsymbol{b}) = \sigma_3 \otimes \boldsymbol{x}_{2n-1}\boldsymbol{y}_{2n-1}.$$

Now, we need to define $H(\boldsymbol{x}_i\boldsymbol{y}_j)$. Before giving the definition, we will introduce the new notation $\boldsymbol{x}\boldsymbol{y}(k, l) \in M$ for simplicity:

$$\boldsymbol{x}\boldsymbol{y}(i, j) := \begin{cases} \boldsymbol{x}_i\boldsymbol{y}_j + \boldsymbol{x}_j\boldsymbol{y}_i & \text{if } i \neq j, \\ \boldsymbol{x}_i\boldsymbol{y}_j & \text{if } i = j. \end{cases}$$

Case 1, if $i < j$:

$$H(\boldsymbol{x}_i\boldsymbol{y}_j) = \begin{cases} \boldsymbol{x}\boldsymbol{y}(i+1, j-1) & \text{if } i = 1 \text{ or } j = 2n-1, \\ \boldsymbol{x}\boldsymbol{y}(i+1, j-1) + \boldsymbol{x}_{j+1}\boldsymbol{y}_{i-1} & \text{otherwise.} \end{cases}$$

Case 2, if $i > j$:

$$H(\boldsymbol{x}_i\boldsymbol{y}_j) = \begin{cases} \boldsymbol{x}\boldsymbol{y}(i-1, j+1) + \rho_{23}\sigma_{23} \otimes \boldsymbol{x}\boldsymbol{y}(i+1, j+1) & \text{if } j = 1 \text{ and } 3 \leq i \leq 2n-3, \\ \boldsymbol{x}\boldsymbol{y}(i-1, j+1) & \text{otherwise.} \end{cases}$$

Case 3, if $i = j$:

$$H(\boldsymbol{x}_i\boldsymbol{y}_j) = \begin{cases} \rho_{23}\sigma_{23} \otimes \boldsymbol{x}_2\boldsymbol{y}_2 & \text{if } i = j = 1, \\ 0 & \text{if } i = j = 2n-1, \\ \boldsymbol{x}_{i+1}\boldsymbol{y}_{j-1} & \text{otherwise.} \end{cases}$$

It is easy to verify that the above map satisfies $G \circ F + \mathbb{I}_M = \delta^1 \circ H + H \circ \delta^1$. $\square$

Remark 5.2. The symmetry of Figure 6 seems to be lost after removing the differentials of the algebra element 1 since the differentials of algebra element $\rho_{23}\sigma_{123}$ are between $\underline{\boldsymbol{x}_{2k}\boldsymbol{b}}$ and $\boldsymbol{x}_{k+1}\boldsymbol{y}_{k+1}$. This phenomenon is caused because we set the map F such that the bottom right corner of the original type-DD structure "collapses." If we set F to collapse the top left corner of the original diagram, then the resulting complex will look like Figure 9.

Acknowledgements

References

[Colin et al. 2011] V. Colin, P. Ghiggini, and K. Honda, "Equivalence of Heegaard Floer homology and embedded contact homology via open book decompositions", *Proc. Natl. Acad. Sci. USA* **108**:20 (2011), 8100–8105. MR Zbl

[Hanselman 2016] J. Hanselman, "Bordered Heegaard Floer homology and graph manifolds", *Algebr. Geom. Topol.* **16**:6 (2016), 3103–3166. MR Zbl

[Hom 2011] J. Hom, *Heegaard Floer invariants and cabling*, Ph.D. thesis, University of Pennsylvania, 2011, available at http://search.proquest.com/docview/878890913.

[Kutluhan et al. 2011] C. Kutluhan, Y.-J. Lee, and C. H. Taubes, "HF = HM, I: Heegaard Floer homology and Seiberg–Witten Floer homology", preprint, 2011. arXiv

[Lipshitz 2006] R. Lipshitz, *A Heegaard–Floer invariant of bordered three-manifolds*, Ph.D. thesis, Stanford University, 2006, available at https://search.proquest.com/docview/304976553.

[Lipshitz et al. 2008] R. Lipshitz, P. Ozsváth, and D. Thurston, "Bordered Heegaard Floer homology: invariance and pairing", preprint, 2008. arXiv

[Lipshitz et al. 2009] R. Lipshitz, P. Ozsváth, and D. Thurston, "Slicing planar grid diagrams: a gentle introduction to bordered Heegaard Floer homology", pp. 91–119 in *Proceedings of Gökova Geometry-Topology Conference 2008*, edited by S. Akbulut et al., Gökova Geometry/Topology Conference, Gökova, 2009. MR Zbl

[Lipshitz et al. 2011] R. Lipshitz, P. S. Ozsváth, and D. P. Thurston, "Tour of bordered Floer theory", *Proc. Natl. Acad. Sci. USA* **108**:20 (2011), 8085–8092. MR Zbl

[Lipshitz et al. 2014] R. Lipshitz, P. S. Ozsváth, and D. P. Thurston, "Computing $\widehat{HF}$ by factoring mapping classes", *Geom. Topol.* **18**:5 (2014), 2547–2681. MR Zbl

[Lipshitz et al. 2015] R. Lipshitz, P. S. Ozsváth, and D. P. Thurston, "Bimodules in bordered Heegaard Floer homology", *Geom. Topol.* **19**:2 (2015), 525–724. MR Zbl

[Manolescu and Ozsváth 2010] C. Manolescu and P. Ozsváth, "Heegaard Floer homology and integer surgeries on links", preprint, 2010. arXiv

[Ozsváth and Szabó 2004a] P. Ozsváth and Z. Szabó, "Holomorphic disks and knot invariants", *Adv. Math.* **186**:1 (2004), 58–116. MR Zbl

[Ozsváth and Szabó 2004b] P. Ozsváth and Z. Szabó, "Holomorphic disks and topological invariants for closed three-manifolds", *Ann. of Math.* (2) **159**:3 (2004), 1027–1158. MR Zbl

[Ozsváth and Szabó 2008a] P. Ozsváth and Z. Szabó, "Holomorphic disks, link invariants and the multi-variable Alexander polynomial", *Algebr. Geom. Topol.* **8**:2 (2008), 615–692. MR Zbl

[Ozsváth and Szabó 2008b] P. S. Ozsváth and Z. Szabó, "Knot Floer homology and integer surgeries", *Algebr. Geom. Topol.* **8**:1 (2008), 101–153. MR Zbl

[Rasmussen 2002] J. A. Rasmussen, "Floer homology of surgeries on two-bridge knots", *Algebr. Geom. Topol.* **2** (2002), 757–789. MR Zbl

[Sarkar and Wang 2010] S. Sarkar and J. Wang, "An algorithm for computing some Heegaard Floer homologies", *Ann. of Math.* (2) **171**:2 (2010), 1213–1236. MR Zbl

JAEPIL LEE
MATHEMATICS DEPARTMENT
YONSEI UNIVERSITY
SEOUL
SOUTH KOREA
jaepil@yonsei.ac.kr

PACIFIC JOURNAL OF MATHEMATICS

Founded in 1951 by E. F. Beckenbach (1906–1982) and F. Wolf (1904–1989)

msp.org/pjm

EDITORS

Don Blasius (Managing Editor)
Department of Mathematics
University of California
Los Angeles, CA 90095-1555
blasius@math.ucla.edu

Paul Balmer
Department of Mathematics
University of California
Los Angeles, CA 90095-1555
balmer@math.ucla.edu

Vyjayanthi Chari
Department of Mathematics
University of California
Riverside, CA 92521-0135
chari@math.ucr.edu

Daryl Cooper
Department of Mathematics
University of California
Santa Barbara, CA 93106-3080
cooper@math.ucsb.edu

Wee Teck Gan
Mathematics Department
National University of Singapore
Singapore 119076
matgwt@nus.edu.sg

Kefeng Liu
Department of Mathematics
University of California
Los Angeles, CA 90095-1555
liu@math.ucla.edu

Jiang-Hua Lu
Department of Mathematics
The University of Hong Kong
Pokfulam Rd., Hong Kong
jhlu@maths.hku.hk

Sorin Popa
Department of Mathematics
University of California
Los Angeles, CA 90095-1555
popa@math.ucla.edu

Jie Qing
Department of Mathematics
University of California
Santa Cruz, CA 95064
qing@cats.ucsc.edu

Paul Yang
Department of Mathematics
Princeton University
Princeton NJ 08544-1000
yang@math.princeton.edu

PACIFIC JOURNAL OF MATHEMATICS